In situ wake measurement behind a 25-kW freewheeling vertical axis hydrokinetic turbine in energetic riverine environment using acoustic Doppler current profiler and acoustic Doppler velocimeter

By

Abbas Dharamsi

A thesis submitted to the Faculty of Graduate Studies of the University of Manitoba
in partial fulfillment of the requirements of the degree of

MASTER OF SCIENCE

Department of Mechanical Engineering
The University of Manitoba
Winnipeg

Abstract

Hydrokinetic turbines present an opportunity for generating renewable energy sustainably in support of microgrids. This research examines the performance and environmental impact of a 25-kW New Energy vertical axis hydrokinetic river turbine under freewheeling conditions, focusing on flow and turbulence behavior. Field measurements of flow velocity at the Canadian Hydrokinetic Turbine Test Center on the Winnipeg River are measured using an acoustic Doppler current profiler and an acoustic Doppler velocimeter. Measurements are taken at various distances downstream of the turbine, from 1 to 17 turbine diameters, to analyze turbulence intensity, turbulent kinetic energy, and mean velocity profiles. The results indicated that turbulence intensity was highest near the turbine, with peaks at the centerline reaching 84% in the first acoustic Doppler current profiler test and 119% in the second, while acoustic Doppler velocimeter measurements showed 41% and 55%, respectively. As expected, turbulence levels gradually decreased with increasing distance from the turbine and are documented. Additionally, the TKE values exhibited a similar trend, demonstrating significant energy dissipation and flow stabilization further downstream. The mean velocity profiles revealed the maximum velocity deficit near the turbine, which gradually recovered with distance. River in-situ values measured do not compare favorably with scaled turbine water tunnel studies. This comprehensive analysis, comparing acoustic Doppler current profiler and acoustic Doppler velocimeter data, provides valuable insights into the wake dynamics and turbulence characteristics of vertical-axis turbines, which are required for optimizing turbine efficiency and assessing environmental impacts.

Acknowledgments

First and foremost, I express my profound gratitude to Dr. Eric Bibeau for providing me with the opportunity to pursue this research and for imparting his extensive knowledge and experience. His guidance has been instrumental in the successful completion of this thesis. I would like to acknowledge Zeev Kapitanker for his significant contributions to the design, maintenance, and operation of the research equipment, both in the laboratory and at the research site. His technical expertise has been indispensable. Additionally, I am grateful to Kirk Dyson for his assistance in data collection and field operations at the CHTTC, which has been vital for this research. I also wish to thank Mitacs for their financial support, which has been essential in facilitating this project. I am deeply thankful to my family for their continuous encouragement, patience, and unwavering support throughout this journey. Their belief in me has been a constant source of motivation. Lastly, I extend my heartfelt thanks to my lab group members, Laëtitia Duret, Ibrahim Aqdiam, Ishan Tandon, and Malcolm Paintin. Their collaboration, camaraderie, and support have played a significant role in the completion of this thesis. Thank you all for being an integral part of this journey.

Contents

List of Figures

Nomenclature

ADCP	Acoustic Doppler current profiler
ADV	Acoustic Doppler velocimeter
CFD	Computation fluid dynamics
CHTTC	Canadian hydrokinetic turbine test center
D	Turbine diameter
DES	Detached eddy simulation
GPS	Global positioning system
HP	Horsepower
HKT	Hydrokinetic turbine
K-ω SST	A type of turbulence model used in CFD simulations
LES	Large eddy simulation
Lest	Estimated wake dissipation length
m	Metres
m/s	Metres per second
RANS	Reynolds-averaged Navier-Stokes equations
TKE	Turbulent kinetic energy
TI	Turbulence intensity
UVW	Instantaneous streamwise, spanwise and vertical velocities
u'v'w'	Fluctuating components of the streamwise, spanwise and vertical velocities
VAHKT	Vertical axis hydrokinetic turbine
WEC	World energy council

Chapter 1

Introduction

The growing global population and the consequent rise in energy demand necessitate the exploration of renewable energy sources. The transition from fossil fuels to renewables is critical to addressing environmental concerns and ensuring energy security. Hydrokinetic energy, as part of the broader renewable energy mix, holds significant potential for contributing to a sustainable energy future.

1.1 World energy demand

According to the United Nations Secretariat (2008), the global population is projected to exceed 8.3 billion by 2030. Correspondingly, energy demand is anticipated to rise from 138.5 TWh to 678 TWh (Energy Information Administration, 2009). This substantial increase in energy consumption indicates that the current rate of energy use could deplete most remaining fossil fuel resources within this century (Manwell et al., 2002) and significantly increase the CO_2 in the atmosphere which is presently at 420 ppm and increasing at 2.6 ppm per annum with new feedback loops potentially increasing this year. Currently, fossil fuels remain the predominant energy source, accounting for 78% of global energy consumption in 2014 (International Energy Agency, 2009). However, the excessive use of fossil fuels has numerous environmental repercussions, including global warming, air pollution, acid precipitation, ozone depletion, forest destruction, and the release of radioactive materials (Dincer, 2000). Moreover, the finite nature of fossil fuel reserves means that renewable energy sources must be developed to meet future energy demands (Kaltschmitt et al., 2007).

Peak fossil fuel production, global warming, and the imperative to shift a significant portion of primary energy sources to renewables are key factors driving the development of renewable energy technologies (Templin and Rangi,

1983). Renewable energy is derived from natural processes such as solar fusion, geothermal fission, and planetary motion (Ocean Renewable Energy Coalition, 2011). A diverse mix of renewable energy solutions will be necessary to replace fossil fuels effectively (Natural Resources Canada, 2011).

Renewable energy contributed 19.2% to global energy consumption by the end of 2014, growing at an annual rate of 2.6%, as reported by the Renewable Energy Policy Network for the 21st Century (REN21) in 2016. Unlike fossil fuels, renewable energy sources have a minimal environmental impact and help reduce global CO2 emissions while adding flexibility to the energy mix by decreasing reliance on limited fossil fuel reserves (Bullard et al., 2013). Various renewable energy sources, including solar, wind, hydro, and biomass, are increasingly replacing fossil fuels (International Energy Agency, 2015). Government policies promoting sustainability, energy security, and cost reduction have narrowed the cost gap between fossil fuels and renewable energy, making many renewable options more economically viable (McGowan, 1990). Researchers, energy companies, and stakeholders are increasingly focused on renewable energy sources to address the growing energy demand and the challenges posed by climate change (Khan et al., 2008).

1.2 Hydrokinetic energy systems

Hydrokinetic energy systems, such as those utilizing river and tidal flows, are gaining attention as emerging renewable energy technologies (Colby and Corren, 2008). These systems, including HKT, convert the kinetic energy of flowing water into electrical energy (Muste et al., 2004). Unlike traditional hydroelectric power that relies on potential energy from dammed water, HKT harness the kinetic energy of free-flowing water, offering lower power densities but greater environmental benefits (Muste et al., 2002).

The significance of hydrokinetic energy lies in its potential to provide a sustainable and consistent source of renewable energy to support microgrids. Water currents are more predictable and less variable than other renewable energy sources like wind and solar power, ensuring a more stable and reliable energy supply (Khan et al., 2009). Moreover, hydrokinetic energy can be generated continuously, day and night, irrespective of weather conditions, thus complementing other renewable energy sources to create a balanced and resilient energy grid (Ebdon et al., 2021).

HKT present a promising alternative for remote communities, such as those in northern Canada, which currently rely on diesel generators for electricity. These turbines not only offer a more cost-effective solution but also provide environmental benefits by reducing greenhouse gas emissions (El-Shamy, 1977). Moreover, HKT can be deployed in various water bodies, including oceans and rivers, making them versatile in their application (Baxter, 1985).

VAHKT are particularly promising due to their ability to capture energy from water flowing in multiple directions, making them suitable for tidal and riverine applications (Salimjira & Khan, 2012). These turbines can operate efficiently at low flow speeds and have a lower environmental impact compared to horizontal axis turbines (Khan et al., 2009). VAHKT also have a simpler design, which can reduce maintenance costs and increase reliability (Salleh et al., 2019).

The integration of hydrokinetic turbines into the energy grid can enhance the diversity and resilience of energy sources. By providing a steady and predictable supply of electricity, hydrokinetic turbines can help balance the intermittency of wind and solar power, contributing to a more stable and robust energy system (Laws & Epps, 2016). Furthermore, the use of hydrokinetic energy can stimulate local economies, create jobs, and promote sustainable development in coastal and riverine communities (Muller & Mueller, 2009).

1.3 Wake measurements

HKT present a promising solution for generating renewable energy by harnessing the kinetic energy of flowing water in rivers and tidal currents. However, the operation of these turbines introduces complex flow dynamics that must be better understood to optimize their performance and minimize their environmental impact. One of the critical aspects of these flow dynamics is the turbulence generated in the wake of the turbine.

1.3.1 Efficiency and performance

When a hydrokinetic turbine operates, it disrupts the flow of water, creating a turbulent wake downstream. This turbulence can lead to several challenges:

- Flow field influence: The turbulent wake affects the flow field around the turbine and any subsequent turbines placed downstream in a hydrokinetic farm. This can lead to reduced energy capture efficiency for downstream turbines, as they operate in a disturbed flow rather than a free stream (Gauvin-Tremblay & Dumas, 2022).
- Energy extraction optimization: Understanding the turbulence helps in optimizing the placement and design of turbines. By strategically positioning turbines to minimize negative interactions from the wake, energy extraction efficiency can be maximized (Chawdhary et al., 2017).
- Mechanical stress reduction: Turbulence can cause fluctuating forces on the turbine blades, leading to mechanical stress and fatigue. By studying the turbulence, engineers can design more robust turbines that can withstand these forces, enhancing their durability and reliability (Chawdhary et al., 2017; Gauvin-Tremblay & Dumas, 2022).

1.3.2 Wake decay

An important aspect of turbulence measurement is understanding wake decay, which refers to the gradual dissipation of turbulence and recovery of flow velocity as the distance from the turbine increases. Measuring wake decay is important because:

- Impact on downstream turbines: The rate at which turbulence dissipates directly affects the performance of downstream turbines in an array. Faster wake decay leads to a quicker recovery of flow conditions, allowing downstream turbines to operate more efficiently (Guerra & Thomson, 2019).
- Optimization of turbine spacing: Accurate measurement of wake decay helps in determining the optimal spacing between turbines. This ensures that downstream turbines experience less turbulence and more stable flow conditions, improving overall array performance (Aghsaee & Markfort, 2018).
- Environmental considerations: Understanding wake decay is also vital for assessing the environmental impact of hydrokinetic turbines. The turbulence and velocity deficits in the wake can affect sediment transport and aquatic habitats. Measuring wake decay helps in designing turbines and deployment strategies that minimize these impacts (Jacobson et al., 2012).

1.3.3 Environmental impact

Integrating hydrokinetic turbines into aquatic environments introduces significant environmental challenges:

- Sediment and nutrient distribution: The turbulence generated by turbines can alter sediment transport and nutrient distribution in the water. This can affect the local aquatic ecosystem by disrupting habitats, altering sediment patterns, and potentially harming species that rely on specific conditions for feeding, spawning, or shelter (Jacobson et al., 2012).
- Ecosystem disruption: High turbulence can cause changes in the water quality and disrupt the natural behavior and lifecycle of aquatic organisms. For

example, fish can experience disorientation and increased vulnerability to predators in highly turbulent areas (Pavlov et al., 1982).

1.3.4 Practical applications of turbulence data

The data collected from turbulence measurements have practical applications in several areas:

- Turbine array layout optimization: The insights gained from turbulence measurements are crucial for determining optimal spacing between turbines in an array. This helps in maximizing power output while minimizing adverse interactions between turbines (Aghsaee & Markfort, 2018).
- Advanced design strategies: Both experimental and analytical studies have demonstrated how turbulence intensity (TI) impacts turbine efficiency. Advanced design and operational strategies can be developed to manage these effects, ensuring consistent and efficient turbine operation (Dhalwala et al., 2022).

1.4 Measurement techniques

This study employs acoustic measurement devices which includes the ADCP and ADV as shown in Figure 1. These devices are particularly suitable for high-energy river environments due to their ability to provide detailed and accurate flow velocity and turbulence measurements. ADCP measure flow velocities over a wide range of depths, offering comprehensive velocity profiles, while ADV provide high-frequency velocity measurements at specific points, allowing for detailed turbulence analysis. The combination of ADCP and ADV ensures a robust and precise understanding of flow dynamics, which is essential for optimizing the performance and environmental compatibility of hydrokinetic turbines.

Figure 1: (Left) SonTek RiverSurveyor M9 ADCP, used for comprehensive flow velocity and discharge measurements across the entire water column (SonTek, 2013). (Right) Nortek Vector 300 m, utilized for high-frequency velocity measurements at specific points (Nortek, 2005).

1.5 Research objectives

The objective of this research is to provide a comprehensive understanding of wake decay measurements behind a freewheeling VAHKT in an energetic river environment through in situ measurements. The specific research objectives are:

1. In situ measurement of wake decay: Conduct in situ measurements of wake decay downstream of a 25-kW vertical axis turbine in an energetic river using ADCP and ADV techniques. This objective aims to capture real-world wake dynamics and compare them with existing computational fluid dynamics (CFD) simulations and water tunnel experiments.
2. Comparison of ADCP and ADV results: Analyze and compare the flow velocity and TI data obtained from ADCP and ADV measurements. This objective will assess the accuracy and reliability of these two measurement techniques in capturing wake characteristics in an energetic river environment.
3. Comparison with CFD and water tunnel studies: Compare the in-situ wake decay measurements with results from CFD simulations and water tunnel experiments conducted in previous studies. This objective aims to identify discrepancies between real-world and simulated wake behaviors, highlighting

the limitations of CFD models and the importance of in situ data for optimizing turbine design and array configurations.

4. Evaluation of environmental impacts: Assess the environmental impacts of the wake generated by the turbine, including effects on sediment transport, aquatic habitats, and water quality. This objective will contribute to developing guidelines for the sustainable deployment of hydrokinetic turbines in river environments.

By achieving these objectives, this research aims to provide valuable insights into the wake dynamics of VAHKT, enhance the accuracy of predictive models, and support the sustainable development of hydrokinetic energy projects.

1.6 Methodology

To achieve project objectives, the methodology was to obtain measurements at the CHTTC in Manitoba, Canada behind a 25-kW New Energy Corporation turbine. The turbine was made available to this project by the First Nation community of Sagkeeng. The CHTTC shown in Figure 2 is known for its high-turbulence flow environment with river boils, which provides an ideal testing ground for hydrokinetic turbines. The site's natural conditions, including fluctuating flow velocities and turbulent characteristics, closely mimic real-world scenarios, thereby enhancing the reliability and applicability of the experimental findings.

The CHTTC was established to offer turbine developers a low-cost opportunity to test their devices in a river environment, in collaboration with researchers at the University of Manitoba. It has attracted significant interest from various HKT companies and now serves as a facility to test prototype designs. This center fosters collaboration between industry and researchers to advance the development of hydrokinetic turbines.

Figure 2: Aerial view of the Canadian Hydrokinetic Turbine Test Center (CHTTC) located near the Seven Sisters Generating Station. The CHTTC, marked by the red pin, is situated in a strategic position for testing hydrokinetic turbines, with proximity to both Jackfish Bay and Whitemouth Falls Provincial Park. The site offers a controlled environment with optimal flow conditions for turbine performance evaluation and research.

However, the Winnipeg River experienced 2 years of drought making the velocity for this study in summer much lower than usual. In addition, the New Energy turbine power electronics was under development and not available during the testing, so tests were conducted in free-wheeling mode.

1.6.1 Location and infrastructure

The CHTTC is located on the Winnipeg River near Seven Sisters, Manitoba, downstream of the Seven Sisters Manitoba Hydro dam. This location is particularly suitable for testing hydrokinetic turbines due to several factors:

- Man-made channel: A portion of the river reach is a man-made channel with an approximately uniform depth, simplifying deployment planning and allowing specific types of turbines to be tested at isolated locations.
- Debris management: The dam upstream removes most debris, and the lack of trees along the channel sides minimizes floating debris such as trees or logs, ensuring reliable turbine operation.
- Variable flow conditions: River flow changes frequently due to environmental conditions and VAR control by operating a powered turbine as a motor, which reduces the flow. This variability allows for testing turbines in different flow speeds.

1.6.2 Site characteristics

The CHTTC site features a man-made channel approximately 1-km long, carved in granite bedrock. It has a width of approximately 60 m and a depth ranging from 9 to 12 m. The flow velocity at the CHTTC ranges from 1.5 to 3.0 m/s, ideal for testing HKT operations. The site's consistent flow conditions are supported by hourly discharge data available from Manitoba Hydro, aiding in correlating turbine performance throughout the HKT operations. The high flow velocity ensures that the channel remains unfrozen even during extremely cold winter conditions, with temperatures dropping to -30°C or lower for several weeks. The high turbulent flow and variable flow rate characteristics attract marine turbine manufacturers and developers looking for life-cycle project solutions and fully grid-integrated systems. The channel's cross-section is nearly rectangular, with right-angle edges and a smooth bed contour, devoid of considerable roughness, large boulders, or hydraulic jumps, making it an excellent testing environment.

1.7 Contributions

The research presented in this thesis provides significant contributions to the field of hydrokinetic energy, particularly in the understanding and optimization of VAHKT. The following key contributions are highlighted:

1.7.1 Enhanced understanding of turbulence characteristics

- Detailed TI analysis: This study provides a comprehensive analysis of TI levels downstream of a VAHKT operating under freewheeling conditions. It demonstrates that TI peaks near the turbine and gradually decreases with increasing distance downstream, providing valuable data for optimizing turbine placement and design in hydrokinetic energy farms.
- Vertical distribution of turbulence: The research reveals significant variations in TI with depth, showing higher turbulence levels near the water surface compared to deeper depths. This finding is crucial for understanding the vertical distribution of turbulence, which is essential for designing turbines that minimize environmental impact and maximize performance.

1.7.2 Technical improvements

- Integration of dual measurement techniques: By utilizing both ADCP and ADV for flow measurements, the study ensures robust and comprehensive data collection. The use of these complementary techniques enhances the reliability of the results and allows for detailed cross-validation, leading to more accurate and insightful findings.
- Focus on freewheeling conditions: The research specifically investigates the turbine's behavior under freewheeling conditions, where it is not connected to an electrical load. This approach provides a baseline understanding of intrinsic flow patterns and turbulence characteristics without the confounding effects of load-induced changes. It serves as a critical reference for future studies under loaded conditions.

1.7.3 Environmental and practical implications

- Mitigation of environmental impact: The study's insights into turbulence characteristics and their impact on sediment transport, aquatic ecosystems, and fish safety are vital for developing environmentally sustainable turbine

designs and deployment strategies. The findings underscore the importance of considering environmental factors in the optimization of hydrokinetic energy systems.

- Optimization of turbine array layouts: The research findings on wake recovery and turbulence decay are essential for determining optimal spacing between turbines in an array. Proper turbine placement can maximize energy extraction efficiency and minimize mechanical stresses and mutual interferences between turbines, leading to more efficient and reliable hydrokinetic energy systems.

1.7.4 Contributions to future research

- Comprehensive dataset for model validation: The turbulence data collected under real-world conditions provide a valuable resource for validating numerical models and simulations. This dataset can improve predictive models, leading to better turbine designs and more accurate assessments of turbine performance in various flow conditions.
- Baseline for further investigations: This research serves as a foundational study for future investigations into the performance of VAHKT under different operational conditions. Future studies can build on this work to explore the effects of loading, varying flow velocities, and other environmental factors, thereby enhancing the overall understanding and application of hydrokinetic energy technologies.

Thus, the research contribution is to advance the understanding of flow dynamics and turbulence characteristics in the wake of VAHKT when they are in operation and subject to large eddies found in energetic rivers. The methodological innovations, environmental considerations, and practical insights provided by this study contribute to the optimization and sustainable deployment of hydrokinetic energy technologies.

1.8 Outline

In the next chapter, the literature review begins with an examination of risk optimization in the context of hydrokinetic energy systems. This includes a detailed discussion on the theory of risk optimization and how it applies to the performance and environmental impact of hydrokinetic turbines. The review then covers various studies on hydrokinetic wakes, highlighting the importance of understanding wake dynamics to optimize turbine efficiency and minimize environmental risks. The chapter also evaluates the potential risks associated with hydrokinetic energy systems, such as impacts on efficiency, environmental disturbances, safety of aquatic life, maintenance challenges, noise and vibration, as well as the influence on flood dynamics.

In the following chapter, the experimental setup and methodologies used in the study are detailed. It begins with a description of the VAHKT used, including its specifications and deployment on a floating pontoon boat. The chapter then explains the acoustic and flow measurement instruments utilized, specifically the ADV and the ADCP. Detailed procedures for data collection, including the positioning and movement of the measurement equipment downstream from the turbine, are provided. The integration of ADV and ADCP data is discussed to ensure comprehensive analysis and validation of the results.

The results chapter presents the findings from the ADCP and ADV measurements. It starts with an analysis of the ADCP data, focusing on streamwise mean velocity, turbulence kinetic energy, and TI. This is followed by a detailed comparison of the ADV results with the ADCP data, highlighting the consistency and reliability of the measurements. The chapter also explores the variability of TI with depth and distance downstream from the turbine. Factors contributing to high TI and its subsequent decay are discussed, providing insights into the wake dynamics of the hydrokinetic turbine.

In the final chapter, the conclusions and recommendations are presented. This chapter summarizes the key findings and provides recommendations to enhance the understanding of wake dynamics and turbulence characteristics in hydrokinetic energy systems.

Chapter 2

Literature review

2.1 Flow measurements in energetic river sites

While there are effective instruments for measuring flow in laboratory environments or slow-moving river segments, these tools and methods are often unsuitable for high-energy river flows where the velocity exceeds 2m/s. Particle image velocimetry, for example, is used to measure flow velocities in controlled, small-scale settings by illuminating seeding particles with a laser and tracking their movements through imaging. However, particle image velocimetry is impractical for HKT sites due to the need for a laser, controlled conditions, seeding particles, and a camera. Introducing particles into natural water flows is environmentally harmful and costly, and a sufficiently powerful laser to cover an entire river section poses safety risks. Moreover, positioning a camera to capture the vertical velocity profile of the flow is complex, as it requires capturing the side plane of the flow. Installing a camera within the riverbank is challenging, and an overhead camera setup would only provide horizontal profiles across the water surface, lacking vertical flow information.

2.2 Turbulence

Turbulence refers to the chaotic, random motion of fluid particles, characterized by vortices and eddies of varying sizes. This disordered motion is a fundamental state for most fluids in natural and engineering systems, especially relevant to hydrokinetic turbines (David, 2016). Turbulence encompasses a wide range of scales, from large eddies where kinetic energy is initially introduced, and down to very small eddies where this energy is eventually dissipated as heat through viscous forces.

Richardson (1922) conceptualized turbulence as a cascade process where energy is transferred from larger to smaller eddies. Large-scale motions are influenced by flow geometry and boundary conditions, which control the transport and mixing within the flow. These large eddies break down into smaller ones, transferring energy until it reaches the microscale level where viscous dissipation occurs (Marcuso, 2012).

The turbulence intensity (TI), defined as the ratio of the root-mean-square of velocity fluctuations to the mean flow velocity, helps quantify the nature of turbulence. It is a crucial factor in designing and analyzing hydrokinetic turbines, as different levels of TI can significantly affect performance. Typically, low TI (less than 1%) is found in controlled laboratory conditions, medium turbulence (1%-5%) in rivers and downstream of turbulence-generating grids, and high turbulence (5%-20%) in fast-flowing rivers (Soltani et al., 2011; Ghorbanian et al., 2011; Strom & Papanicolaou, 2007; George et al., 1994; Nikora and Smart, 1997).

In riverine environments, turbulence is driven by the interaction of the flow with various natural and man-made features, such as meanders, obstacles, and channel geometry. These interactions produce eddies of various sizes, contributing to the overall turbulent flow structure. The large-scale turbulence in rivers is influenced by the geometry of the river, including its depth and width, while smaller scales are associated with viscous dissipation and energy transfer within the flow (Brocchini, 2015).

To quantify and analyze turbulence in fluid flows, several key metrics are used:
3D Turbulent Intensity: The three-dimensional TI is a measure of the magnitude of velocity fluctuations in all three spatial directions. It is calculated using the root mean square of the velocity fluctuations (u′, v′, w′) in the streamwise, transverse, and vertical directions, respectively. The formula for 3D TI is:

$$TI = \frac{\sqrt{\frac{1}{3}(u'^2+v'^2+w'^2)}}{\sqrt{\bar{u}^2+\bar{v}^2+\bar{w}^2}}$$

Where $\bar{u}$, $\bar{v}$, and $\bar{w}$ are the mean velocities in the respective directions.

Streamwise turbulent intensity: The streamwise turbulent intensity focuses on the velocity fluctuations in the direction of the flow. It is defined as the ratio of the standard deviation of the streamwise velocity fluctuations to (σ_u) the mean streamwise velocity $(\bar{u})$

$$TI = \frac{\sigma_u}{\bar{u}}$$

TKE: TKE represents the energy contained in the turbulent eddies of the flow. It is computed as:

$$TKE = \frac{1}{2}(\bar{u'^2} + \bar{v'^2} + \bar{w'^2})$$

where $\overline{u'^2}$, $\overline{v'^2}$, and $\overline{w'^2}$ are the mean squares of the velocity fluctuations in the respective directions.

These metrics provide a comprehensive understanding of the turbulence characteristics in a fluid flow, essential for optimizing the performance and design of hydrokinetic turbines and other fluid systems.

2.3 Turbulence effects

The demand for renewable power generation has become increasingly critical as the world's energy consumption is anticipated to surge by over 70% in the next three decades, driven by population growth and rapid industrialization (Jennings, 1996). The shift towards renewable energy is part of a broader quest for sustainable development, which aims to balance economic growth with environmental preservation (WCED, 1987). Traditional energy generation methods, which heavily depend on finite and polluting fossil fuels like coal, natural gas, and petroleum, are now recognized as unsustainable due to their substantial

contributions to global warming (World Energy Council, 2016). Thus, the development of renewable energy sources, especially hydrokinetic turbines, is essential for achieving energy independence from fossil fuels and mitigating the environmental impacts of traditional energy production (IPCC, 2022). Hydrokinetic turbines generate electricity by harnessing the kinetic energy of flowing water (Ibrahim et al., 2021). Their use in rivers offers several benefits, including minimal infrastructure requirements and sustainable operation (Khan et al., 2020). However, their installation and operation in natural environments create complex interactions that need careful optimization to minimize potential risks (Liu et al., 2019).

This study provides a comprehensive literature review on the wake effects of hydrokinetic turbines, analyzed through the perspective of risk optimization theory. Wake effects refer to the flow disturbances caused by turbine operation and are vital for understanding both the environmental impact and efficiency of these energy systems (Zhang et al., 2020). By applying a risk optimization framework to the analysis of wake effects, it is possible to systematically identify, evaluate, and optimize the risks associated with wake dynamics (Aven, 2016). The primary aim of this review is to synthesize current research on the wake characteristics of hydrokinetic turbines and assess how these characteristics influence turbine performance and environmental outcomes. By using a risk optimization perspective, this review seeks to identify potential hazards and operational challenges resulting from wake effects, offering insights into how these risks can be anticipated and optimized (Aven, 2016). By highlighting the risks associated with the deployment and operation phases of hydrokinetic turbines, this paper underscores the need to improve both the reliability and effectiveness of these systems while minimizing their environmental footprint. The findings from this literature review will provide a foundation for future research and development efforts in the field, aiming to optimize hydrokinetic

energy systems that balance technological advancements with ecological sensitivity.

2.3.1 Risk optimization theory

Risk optimization theory focuses on identifying, assessing, and managing uncertainties and potential negative outcomes related to specific actions or decisions, with the goal of finding the best balance between risk and reward (Lin & Lu, 2023). It aims to quantify and mitigate risks to improve decision-making processes and outcomes (Aven, 2016). In the context of hydrokinetic energy systems, applying risk optimization involves evaluating the technical, environmental, and operational risks associated with VAHKT. This includes the potential for equipment failure, environmental disruption, and unforeseen operational challenges (Snowberg & Weber, 2015). Recognizing these complexities and working towards solutions that balance human needs with environmental protection is essential. This can involve designing more environmentally friendly turbines, carefully selecting turbine locations, or developing new technologies that minimize the risks associated with downstream turbulence. By pre-emptively identifying and optimizing these risks, project developers can enhance reliability, efficiency, and environmental stewardship (Aven, 2016).

2.3.2 Hydrokinetic wakes

A significant feature of hydrokinetic energy systems is the formation of a wake, characterized by swirling fluid movements after water passes through a turbine (Lago et al., 2010). This wake is marked by a reduced mean flow velocity caused by the turbine structure and the energy extraction process (dos Santos et al., 2021). For the wake to exist, the rotor must experience fluid drag, which occurs due to momentum loss from initial velocity reduction, intense pressure gradients, and vortex structures (Chamorro & Porté-Agel, 2009). The velocity within this

wake takes time to recover, impacting the hydrokinetic power output, which is directly related to flow velocity (dos Santos et al., 2021).

The wake is characterized by turbulence involving chaotic flows with the formation of eddies and vortices (Posa & Broglia, 2021). This turbulence can substantially impact the flow field around the turbine and those downstream, affecting their operational efficiency and environmental impact (Gauvin-Tremblay & Dumas, 2022). Strategically positioning turbines and understanding wake effects are essential for optimizing energy extraction and reducing mechanical stress on turbine structures (Nash et al., 2021). Research indicates that an appropriate spatial layout and a thorough understanding of wake dynamics can improve turbine efficiency and array performance (Chawdhary et al., 2017; Zhang et al., 2020).

Arranging and spacing new hydrokinetic turbines within a water body necessitates a comprehensive understanding of wake behaviors and their dissipation lengths (Guerra & Thomson, 2019). Precisely identifying the areas where velocity and energy recover is critical for optimizing turbine layouts (Nash et al., 2021). Furthermore, the dissipation of turbulent structures within the wake must be considered, as these can influence the performance of subsequent turbines (Chawdhary et al., 2017). The extent to which the wake dissipates is vital in determining the density and placement of turbines, affecting energy capture and the overall economic viability of the hydrokinetic farm (dos Santos et al., 2021).

2.3.3 Efficiency and performance

The turbulence created downstream of a turbine can significantly influence the flow field around it and subsequent turbines in a hydrokinetic energy farm (Gauvin-Tremblay & Dumas, 2022). Gaining an understanding of this turbulence is essential for optimizing turbine placement and design, which in turn maximizes energy extraction efficiency and reduces mechanical stresses on the turbines

(Chawdhary et al., 2017). This understanding is critical for enhancing the overall durability and reliability of the energy systems, thereby extending their operational lifespan and improving their economic viability (Gauvin-Tremblay & Dumas, 2022).

The strategic deployment and arrangement of hydrokinetic turbines in arrays are vital for enhancing energy extraction and effectively meeting community energy demands (Chawdhary et al., 2017). This study emphasizes that spatial arrangement plays a crucial role in maximizing the operational efficiency of these turbines (Chawdhary et al., 2017). Central to understanding the dynamics within these arrays is the concept of the wake effect (Zhang et al., 2020). This phenomenon encompasses the impact of upstream turbines on the flow dynamics and energy-capture capabilities of downstream units (Ikhsan & Fachri, 2023). Research shows that wake development can result in significant momentum loss and flow irregularities, consequently decreasing the electricity production capacity of downstream turbines (Zhang et al., 2020).

However, the adverse impacts associated with the wake effect can be mitigated. Optimizing the spatial layout of turbine arrays can significantly enhance power output under certain configurations (Park & Law, 2015). This optimization requires careful planning of the positions and distances between turbines to minimize adverse interactions and maximize the beneficial flow characteristics for power generation (Aghsaee & Markfort, 2018). Additional insights into these dynamics have been provided by 3D computational simulations, which have explored how turbulence, blockage effects, and other related processes are influenced by the positioning of upstream rotors relative to downstream units (Mycek et al., 2014).

Furthermore, the optimization of hydrokinetic turbine arrays is complicated by the influence of TI on turbine efficiency (Gauvin-Tremblay & Dumas, 2022).

Oscillations in power output caused by turbulent inflow conditions present a significant challenge to maintaining consistent and efficient turbine operation (Forbush et al., 2019). Both experimental and analytical studies have demonstrated how TI can impact the overall efficiency of hydrokinetic turbines, highlighting the need for advanced design and operational strategies to manage these effects (Dhalwala et al., 2022).

Collectively, these studies underscore the complex nature of designing and operating hydrokinetic turbine arrays. They emphasize the necessity of an integrated approach that incorporates both spatial arrangement and dynamic interactions within the turbine system. This integration is crucial for optimizing energy output and mitigating operational risks related to turbulence and wake effects.

2.3.4 Environmental impact

Integrating hydrokinetic turbines into aquatic environments poses substantial environmental challenges, particularly in terms of sediment and nutrient distribution (Ross et al., 2021). The turbulence induced by these turbines can disrupt local aquatic ecosystems (Jacobson et al., 2012), highlighting the need to understand turbulence characteristics for developing environmentally friendly turbine designs and deployment strategies. By thoroughly investigating these turbulence characteristics, developers can devise turbine designs and strategies that minimize environmental disturbances, promoting a more sustainable integration of hydrokinetic turbines into aquatic systems.

A key impact of turbine installation is the alteration of bed form kinematics. Research has demonstrated that axial-flow turbines in river channels can change local sediment patterns and affect broader sediment transport processes (Hill et al., 2016; Lin et al., 2024). This indicates that turbines influence not only their immediate surroundings but also larger geomorphological dynamics, potentially

altering the shape and migration of sediment bed forms (Hill et al., 2016). Moreover, these effects can be extensive, with variations in suspended sediment concentrations observed up to 15 rotor diameters downstream from the turbine (Ramírez-Mendoza et al., 2018). This significant influence suggests that the wake of a turbine can impact sediment distribution over considerable distances, potentially affecting the efficiency of turbine arrays and altering coastal sediment transport dynamics (Ramírez-Mendoza et al., 2018).

The ecological consequences of changes in sediment transport are diverse. Alterations in sediment dynamics are essential for shaping aquatic habitats, with potential habitat loss or modification impacting species dependent on these environments for critical life processes such as spawning, feeding, and shelter (Hauer et al., 2018). Additionally, sediment acts as a carrier for nutrients, pollutants, and organic matter, meaning that changes in sediment transport can directly influence water quality (Lee and Oh, 2018). This has downstream effects on drinking water supplies, recreational water use, and overall aquatic ecosystem health (Hauer et al., 2018).

Furthermore, many aquatic organisms, including fish, have life cycles and behaviors intricately linked to sediment movement and deposition (DFO, 2000). Disruptions to sediment transport can interfere with these natural cycles, potentially leading to reduced biodiversity and altered community structures within aquatic environments (DFO, 2000). This underscores the need for careful consideration and mitigation strategies to ensure the sustainability of these renewable energy solutions within their environmental contexts.

2.3.5 Fish and aquatic life safety

Integrating hydrokinetic turbines into aquatic environments requires a detailed understanding of their impact on local wildlife, especially fish populations. Comprehensive studies are vital to determine the full range of effects these

turbines have on both individual species and broader fish communities (Evans et al., 2009). Historical data indicate that traditional turbine designs have frequently caused significant ecological disturbances, highlighting the urgent need for innovative fish-friendly turbine technologies that minimize ecological footprints (Jacobson et al., 2012).

The mechanical aspects of hydrokinetic turbines, including their operation at high speeds and specific structural features, introduce shear and turbulence into aquatic habitats (Killgore et al., 2001). These conditions can pose severe risks to aquatic life, exposing fish to forces that can result in a spectrum of injuries, from minor to fatal (Neitzel et al., 2000). Compelling evidence shows that high shear and turbulence levels can cause anything from minor injuries to lethal damage (Killgore et al., 2001; Neitzel et al., 2000; Čada et al., 1997). Additionally, the turbulence generated by these turbines can lead to fish disorientation (Pavlov et al., 1982). As fish navigate past the turbine equipment, varying sizes of turbulence can increase their vulnerability to predators and disrupt normal population dynamics (Pavlov et al., 1982). Studies have demonstrated a negative correlation between TI and the critical swimming velocities of fish, indicating that excessive turbulence can hinder their ability to navigate and forage effectively (Čada et al., 1997; Pavlov et al., 1982).

Moreover, the placement and size of turbine arrays can significantly impact fish migration patterns (Coutant & Whitney, 2000). Large arrays, especially those with numerous turbines, can create barriers that impede the natural movement of fish, particularly larger and predatory species (Copping et al., 2021). This can lead to changes in habitat use and potentially reduce biodiversity within these ecosystems (Coutant & Whitney, 2000). Addressing these impacts requires designing turbines that not only meet energy demands but also incorporate features that protect the aquatic environments they occupy. This approach is essential for balancing the

benefits of renewable energy with the preservation of marine and riverine biodiversity.

2.3.6 Maintenance and durability

Grasping the effects of turbulence on hydrokinetic turbines is essential for enhancing their durability and efficiency in dynamic riverine settings (Muratoglu & Yuce, 2017). The turbulence produced during turbine operation can cause considerable wear and tear on turbine components, compromising their durability and necessitating more frequent maintenance (Woods, 2017). This knowledge is crucial for designing turbines that are not only more robust but also require less maintenance, thereby lowering operational costs and minimizing downtime (Sutherland & Kelley, 1995).

Additionally, the interaction between turbines and large-scale turbulent eddies introduces further complexities. Such turbulence can create non-uniform inflow conditions on downstream turbines, leading to increased fatigue loads (Lee et al., 2011). These scenarios underscore the necessity of managing risks associated with potential structural damage within turbine arrays (Sutherland and Kelley, 1995). Research highlights the need for a sturdy turbine design capable of withstanding the dynamic and often harsh conditions present in riverine environments (Zeiner-Gundersen, 2015). Effective designs must address the risks linked to material fatigue, mechanical failure, and efficiency losses that arise under varying flow conditions (Niebuhr et al., 2019). By focusing on these aspects, turbines can be optimized to endure environmental stresses while maintaining high performance levels, ensuring their long-term functionality and reliability (Sutherland & Kelley, 1995).

2.3.7 Noise and vibration

The functioning of hydrokinetic turbines generates noise and vibrations that can greatly affect underwater environments as well as surface activities (Dang et al.,

2019). This turbulence-induced noise has the potential to impact both aquatic and human life, highlighting the need for designing quieter turbines that reduce disruption (Bevelhimer et al., 2016). Research conducted by Wang et al. (2007) demonstrated that turbine noise, particularly when severe cavitation is present, can disturb the environment, leading to sediment disruption and negatively affecting marine life near the seabed.

The broader ecological impacts of turbine noise are significant, given the sensitivity of numerous marine and freshwater animals to sound (Schramm et al., 2017). These organisms depend on acoustic signals for essential activities such as reproduction, feeding, predator avoidance, communication, and navigation (Popper, 2003). The noise produced during the installation and operation of hydrokinetic devices can pose serious threats to these vital behaviors (Weilgart, 2007). Studies have shown that such noise can cause temporary or permanent hearing loss in marine life, with some cases resulting in physical damage such as balance impairments (Bailey et al., 2010; Würsig & Greene, 2002).

Moreover, the noise from these turbines has been linked to increased stranding events of large marine wildlife, indicating a troubling rise in underwater noise pollution that significantly impacts larger marine animals (Liebschner et al., 2016; Frid et al., 2012). Even lower magnitude noises typical of normal turbine operations can disrupt behaviors and cause physiological stress in marine mammals, sea turtles, and fish (CSA Ocean Sciences Inc., 2023). These disturbances might lead to decreased foraging efficiency, habitat abandonment, reduced reproduction rates, and higher mortality, potentially resulting in adverse effects on both individual organisms and entire populations (NRC, 2005). Given these findings, it is evident that the environmental design and operational strategies of hydrokinetic turbines must prioritize noise reduction to mitigate their impact on marine ecosystems and ensure the coexistence of renewable energy technology with marine and freshwater habitats.

2.3.8 Limited river data

Obtaining adequate wake data from operational hydrokinetic turbines in real river environments remains a major challenge in renewable energy research (Nago et al., 2022). This lack of in situ data makes it difficult for researchers and engineers to accurately forecast and enhance the performance and environmental impacts of turbine installations (Pyakurel et al., 2017). As a result, there is a pressing need for advanced simulation models and experimental setups to bridge the gap between theoretical predictions and real-world conditions.

Due to the logistical and financial challenges associated with deploying measurement equipment in operational river environments, many studies on hydrokinetic turbine arrays depend on lab-scale models and numerical simulations (Brandized et al., 2019; Zhang et al., 2020; Ji et al., 2018). While these methods provide valuable insights, they cannot fully replicate the complex flow dynamics found in actual rivers. Laboratory settings can offer some data on TI measured behind a scaled-down turbine model (Liu et al., 2019). However, these controlled environments struggle to mimic the velocities and eddy formations that occur downstream of an operational turbine in a river (Ji et al., 2018). Real-world rivers display a broader range of flow velocities and naturally occurring turbulence patterns that are difficult, if not impossible, to perfectly replicate in a lab setting (Eltner et al., 2020). This limitation can lead to inaccurate predictions of turbine wake interactions within an array, potentially hindering the optimization of array layouts for maximum energy production.

The lack of methodologies and wake dissipation data from riverine environments, which are crucial for optimizing the arrangement of hydrokinetic turbines, represents a significant obstacle to the progress of hydrokinetic energy generation (Tiago Filho et al., 2017). Recognizing the vital importance of wake dynamics in hydrokinetic farms, this study aims to enhance the understanding of wake

phenomena through detailed experimental analysis. It specifically examines the behavior and dissipation lengths of wakes generated by VAHKT.

2.3.9 Influence on flood dynamics

Installing hydrokinetic turbines in flowing water bodies like rivers naturally alters flow dynamics by creating an obstruction that introduces a drag force (Abutunis, 2020). This drag under subcritical flow conditions can cause notable changes in water levels—raising levels upstream (backwater) and lowering them downstream (drawdown) of the turbine (Jager & Wickman, 2019). Such modifications can significantly affect water management systems, particularly in rivers and canals used for irrigation, by disrupting water supply operations due to altered head-discharge conditions and potentially increasing flood risks from elevated upstream water levels (Gunawan et al., 2017).

Additionally, the ability of rivers to manage floodwaters can be impacted by the installation of hydrokinetic turbines, especially during flood events (Gu & Lei, 2023). The wake and turbulence produced by these turbines could modify flow dynamics, possibly reducing the river's efficiency in managing floodwaters and heightening the risk of flooding in both upstream and downstream areas (Gu & Lei, 2023). Furthermore, the volume of water in canals and rivers fluctuates seasonally due to factors like seasonal rainfall and irrigation demands, influencing the availability of hydrokinetic resources (Gunawan et al., 2017). If not carefully considered, local hydrodynamic changes caused by turbine installation could lead to undesirable events such as flooding, silting, and scouring (Gunawan et al., 2017). Therefore, these complex dynamics must be thoroughly evaluated in the design, operation, and development strategies of hydrokinetic energy projects to ensure they align with existing water resource management practices and do not worsen flood risks or cause other adverse impacts.

While the integration of hydrokinetic turbines into river environments holds great potential for sustainable energy development, it also presents intricate challenges that necessitate thorough optimization and innovative solutions. This paper has examined the diverse impacts of hydrokinetic turbines, with a particular emphasis on wake effects and related risks, using a stringent risk optimization framework.

The examination of wake effects reveals the complex dynamics between turbine operation and environmental interactions. These effects influence not only the operational efficiency of the turbines but also have substantial ecological impacts on river ecosystems. As discussed, the turbulence generated by these turbines can cause sediment redistribution, alter habitat structures, and potentially harm aquatic life. These findings underscore the essential need for designing turbines that minimize environmental disturbances while maximizing energy production.

Additionally, this review has identified a significant gap in the empirical data required for optimizing turbine design and placement. The scarcity of real-world river data on wake effects presents a considerable challenge, prompting researchers to rely on lab-scale models and simulations that may not fully capture the complexities of natural environments. This gap highlights the urgent need for improved data collection methodologies and advanced modeling techniques that can more accurately simulate real-world conditions.

The insights gained from this literature review provide a strong foundation for ongoing and future research efforts in the field. These efforts can drive the development of hydrokinetic energy systems that are not only technologically advanced but also in harmony with ecological preservation goals. By continually refining risk optimization strategies and enhancing the design and deployment of hydrokinetic turbines, it is feasible to achieve a balance between the advancement of renewable energy and environmental conservation.

2.4 Wake measurements behind hydrokinetic turbines

Understanding the wake dynamics behind hydrokinetic turbines is essential for optimizing turbine array configurations and minimizing environmental impacts. This literature review covers various types of hydrokinetic turbines, including VAHKT, horizontal axis turbines, small-scale turbines in water tunnels, and CFD simulations. The review provides detailed insights into the methodologies, findings, and implications of various studies on wake dissipation, turbulence intensities, and other wake characteristics.

2.4.1 Vertical axis turbines

Chamorro et al. (2015) conducted experimental studies on a VAHKT with a diameter of 0.5 m. The study observed complex wake behaviors, including non-monotonic velocity deficits within the near wake region. The velocity deficit increased monotonically beyond 4 D turbine diameters downstream, indicating the persistence of turbulent structures that affect downstream turbines' performance. The study emphasized the importance of understanding wake interactions for optimal turbine placement and energy capture efficiency.

Critical analysis: Chamorro et al.'s methodology lacked the comprehensive depth of the current study. Their focus was limited to a 0.5 m turbine and did not explore the freewheeling conditions or utilize a combination of ADCP and ADV measurements for a detailed analysis of TI at various distances. The current study used a 25-kW VAHKT, providing a more extensive dataset with measurements taken from 1-17 turbine diameters downstream. This broader range and higher power capacity turbine allowed for a more thorough understanding of wake dynamics under real-world conditions.

Hill et al. (2020) investigated a dual rotor tidal turbine model, revealing that wake dissipation length varied significantly between the left and right rotors. The study found a dissipation length of 10 D for 89% velocity recovery in the left rotor and

84% in the right rotor. This dual rotor configuration showed improved wake recovery compared to single rotor designs, suggesting potential benefits in using multi-rotor systems for tidal energy conversion.

Critical analysis: While Hill et al.'s study provided valuable insights into dual rotor configurations, it did not address VAHKT or use ADCP and ADV techniques to validate their findings. The current research focused specifically on VAHKT and employed both ADCP and ADV measurements to ensure accuracy and depth in TI data. Furthermore, the dual rotor setup was not directly comparable to single rotor freewheeling conditions, which are critical for understanding baseline wake characteristics.

2.4.2 Horizontal axis turbines

Tedds et al. (2014) conducted experimental tests on a 0.5 m diameter horizontal axis turbine in a high-velocity water recirculation channel. The study showed that at 7 D downstream, the flow velocity recovered to approximately 80% of the upstream velocity. The wake characteristics were influenced by the number of blades and flow conditions, demonstrating the necessity of considering these factors in turbine design and placement.

Critical analysis: Tedds et al. focused on a smaller scale turbine and did not employ a range of advanced measurement techniques as the current study did. The current research on a larger 25-kW VAHKT with measurements from 1-17 turbine diameters provided more detailed insights into the wake dynamics. Additionally, the use of both ADCP and ADV allowed for cross-validation and a more nuanced understanding of TI variations.

Myers & Bahaj (2009) investigated the wake properties of a 0.8 m diameter marine turbine through experimental studies. The study found that 80% of the initial velocity was recovered at a longitudinal distance of 10 D. The high turbulence

levels near the turbine made it difficult to determine wake properties accurately, underscoring the importance of considering TI in wake studies.

Critical analysis: Myers & Bahaj's study, focusing on a smaller turbine, did not employ the advanced measurement techniques used in the current research. This study used a larger 3.4 m diameter 25-kW VAHKT and combined ADCP and ADV measurements for a more detailed and validated analysis of TI and wake recovery. The extended measurement ranges from 1-17 turbine diameters also provided a more comprehensive understanding of wake dynamics.

Mycek et al. (2014a) and Mycek et al. (2014b) studied the effects of TI on the wakes of a 0.7 m diameter tidal turbine. The experimental tests revealed that higher TI (15%) resulted in faster wake dissipation, with complete flow recovery at distances close to 6 D. The study also found that for two turbines, higher turbulence conditions improved the overall efficiency of the hydrokinetic park.

Critical analysis: Mycek et al.'s study, while valuable for understanding the effects of TI, did not cover VAHKT or use a combination of ADCP and ADV measurements for validation. The current research focused specifically on VAHKT and employed both ADCP and ADV measurements to provide a more comprehensive and accurate dataset. The larger 25-kW VAHKT and extended measurement range also offered a more detailed analysis of TI and wake recovery.

2.4.3 Small-scale turbines in water tunnels

Nuernberg and TAO (2018) studied the wake behavior of four tidal hydrokinetic turbines with 0.28 m diameter blades in a circulating water channel. The experiments tested various lateral and longitudinal spacing configurations. Results indicated that shorter lateral spacing decelerated velocity recovery, while optimized lateral spacing accelerated wake dissipation. Longitudinal spacing had

a lesser effect. The study found that a single turbine's wake recovered about 72% of the free current velocity at 9 D and 85% at 20 D.

Critical analysis: Nuernberg and TAO's study, conducted in a controlled water channel, did not fully replicate real-world conditions. The current research was conducted at the CHTTC under natural flow conditions, providing more accurate and applicable data. Additionally, the study used a larger 25-kW vertical axis turbine and combined ADCP and ADV measurements for a more detailed analysis of TI and wake recovery.

Chawdhary et al. (2017) investigated a triframe configuration of three 0.15 m diameter axial turbines in an open channel. The setup included one turbine in the front row and two in the second row. The study revealed that the velocity recovery at 8 D was around 80% for all turbines, with the triframe configuration showing higher recovery rates than a single turbine. This arrangement was recommended for hydrokinetic park planning due to its efficient wake management.

Critical analysis: Chawdhary et al.'s focus on small-scale axial turbines in a controlled environment limited the applicability of their findings to larger, real-world scenarios. The current study used a 25-kW VAHKT and conducted measurements in a natural river environment, providing more relevant data for practical applications. The combination of ADCP and ADV measurements also offered a more comprehensive analysis of wake dynamics and TI.

Musa et al. (2018) conducted experimental tests on a 0.15 m diameter axial turbine to observe the relationship between hydrokinetic use and river bottom morphology. The study found that the wake dissipation length was 6 D for 81% recovery of the initial speed. This research provided insights into the interactions between turbine wakes and sediment transport, essential for sustainable river turbine installations.

Critical analysis: Musa et al.'s small-scale experiments did not fully capture the complexities of real-world hydrokinetic turbine operations. The current research, using a larger 25-kW VAHKT and conducted in a natural river environment, provided more accurate and comprehensive data. Additionally, the use of both ADCP and ADV measurements ensured a detailed and validated analysis of TI and wake recovery.

2.4.4 CFD simulations

Silva et al. (2016) performed CFD simulations on a horizontal axis hydrokinetic turbine with three 10 m diameter blades using the ANSYS CFX software. The k-ω SST turbulence model was employed to capture the helical wake structure. The study found that the near wake extended up to 3 D, while the far wake reached 12 D, where the axial velocity fully recovered. This extensive recovery length highlights the need for careful spacing in turbine arrays to minimize wake interactions.

Critical analysis: Silva et al.'s reliance solely on CFD simulations without experimental validation poses limitations on the real-world applicability of their findings. While CFD models can predict flow behavior under controlled conditions, they often fail to account for the complex and variable conditions encountered in natural environments. This lack of field validation means that the results may not fully capture the nuances of real-world wake dynamics, potentially leading to inaccuracies when applied in practice. The current study's field measurements using ADCP and ADV provide critical empirical data, which can be used to compare and validate results from CFD simulations, ensuring a more accurate and robust analysis of wake recovery and TI in actual operating conditions.

Riglin et al. (2016) used Reynolds-averaged Navier-Stokes (RANS) equations in the ANSYS FLUENT software to characterize the influence of turbine wakes on a

hydrokinetic park. The study involved a hydrokinetic micro turbine with three matrix configurations. The findings indicated that the wake dissipated laterally at 2.5 D and longitudinally at 6 D. Downstream turbines were found to be at least 80% less efficient than a single turbine under similar conditions.

Critical analysis: While Riglin et al. study offers valuable insights into the behavior of micro turbine arrays, the exclusive use of CFD simulations without field data significantly limits the study's real-world relevance. CFD simulations, although useful, cannot fully replicate the complex environmental conditions that affect turbine performance in natural settings. The absence of field validation raises concerns about the accuracy of the simulated wake dissipation and efficiency losses. The current research's field measurements using ADCP and ADV offer a more comprehensive analysis of wake behavior under real-world conditions, and the dataset can be used to compare with CFD results to enhance the reliability and applicability of the findings.

Ibarra et al. (2014) utilized CFD simulations to analyze the wake of a horizontal axis turbine with four flat blades. Using the k-ω SST turbulence model in ANSYS FLUENT, the study demonstrated that the wake flow recovered velocity gradually over 8 D, with significant improvements in flow stability and reduced turbulence. The study's velocity contour results provided insights into the wake dynamics essential for optimizing turbine spacing.

Critical analysis: Ibarra et al.'s use of CFD simulations without field validation limits the practical applicability of their findings. While the simulations offer detailed visualizations of wake flow, they are based on assumptions that may not hold true in real-world environments, where factors such as varying flow conditions, environmental turbulence, and material properties play critical roles. The current study's field measurements using ADCP and ADV provide a more robust and accurate representation of wake dynamics and can serve as a valuable

dataset for comparing with CFD results. The research extended the measurement range to 17 turbine diameters, offering a more comprehensive analysis of TI and wake recovery, making the findings more applicable to practical turbine design and optimization.

Santos et al. (2021) conducted a CFD study on a three-bladed hydrokinetic turbine in the Amazon River. The actuator disk model in ANSYS FLUENT was used, incorporating real geometry data and velocity profiles. The study found that wake dissipation varied with turbine performance, with the most efficient configuration showing a dissipation length of 7.3 D. This study highlighted the importance of operating turbines at maximum efficiency to reduce wake interactions and enhance energy capture.

Critical analysis: Santos et al.'s study, while informative, did not include field measurements to validate their CFD findings. This omission limits the reliability of their conclusions, as CFD models can only approximate real-world conditions. The absence of empirical data means that their findings may not fully capture the environmental variables and complexities that influence turbine performance in natural settings. The current study's field measurements offer a more accurate and comprehensive analysis of wake dynamics, and the dataset can be used to compare with CFD simulations to provide validation and refinement. Additionally, the focus on a larger 25-kW VAHKT and a broader measurement range from 1-17 turbine diameters offers more detailed insights into TI and wake recovery, making the results more relevant for practical applications.

Brasil Jr et al. (2016) simulated an axial turbine with four 2 m diameter blades using CFD tools to analyze wake interactions in a river environment. The results indicated a small dissipation around 1.2 D and a near wake persisting up to 8 D. The study also found that a lateral distance of 2.27 D and a longitudinal distance of 1.67 D were sufficient for the installation of a second turbine row.

Critical analysis: Brasil et al. reliance on simulations without field validation limits the applicability of their findings to real-world conditions. While their CFD models offer predictions of wake interactions, these predictions may not fully capture the dynamic and variable nature of actual river environments. The lack of empirical validation raises concerns about the accuracy of their results when applied to real turbine installations. The current study's field measurements using ADCP and ADV provide a more accurate and validated dataset, which can be compared with CFD results to enhance their applicability. The larger 25-kW VAHKT and extended measurement range also offer a more comprehensive analysis of wake dynamics and TI, ensuring that the findings are more applicable to real-world turbine operations.

Leroux et al. (2019) carried out a mathematical study on the velocity deficit in the wake of a horizontal axis tidal turbine using quasi-stationary and transient numerical approaches. The study found that the transient approach provided more physically accurate wake behavior. The velocity deficit ranged from 60% at 2 D to 30% at 10 D for the quasi-stationary approach and from 80% to 50% for the transient approach.

Critical analysis: Leroux et al.'s study, while valuable for understanding numerical approaches, lacked field validation. This absence of empirical data limits the reliability of their conclusions, as numerical models, even when sophisticated, cannot fully replicate the complexities of real-world conditions. The current study's field measurements using ADCP and ADV provide a more robust and accurate dataset, which can be used to compare with CFD simulations to validate and refine the numerical models. The larger 25-kW VAHKT and extended measurement range also offer a more comprehensive analysis of TI and wake recovery, ensuring that the results are more applicable to practical turbine deployment and optimization.

Ouro et al. (2019) used the Large-Eddy Simulation (LES) model to study the impact of turbine arrangement on a tidal turbine hydrokinetic park. The study considered a single row of three turbines and found that the wake dissipation length ranged from 10 D to 12 D. When considering two rows of turbines, the efficiency of the second group was about 30% lower, suggesting the need for greater spacing between rows.

Critical analysis: Ouro et al.'s reliance on LES models without experimental validation limited the practical applicability of their findings. LES models, while powerful, rely on assumptions that may not hold true in the variable conditions of natural environments. Without field data to validate these models, the results may not fully capture the complexities of turbine interactions in real-world settings. The current study's field measurements using ADCP and ADV provide a more accurate and validated dataset, which can be compared with CFD simulations to ensure more reliable results. Additionally, the focus on a larger 25-kW VAHKT and a broader measurement range from 1-17 turbine diameters offered more detailed insights into TI and wake recovery, making the findings more applicable for practical turbine array design.

Richmond et al. (2015) performed a numerical analysis using the DES model to study the wake generated by a 4.88 m diameter marine turbine. The study compared CFD results with ADCP measurements and found that the wake was not fully recovered until 12 D. The results highlighted the challenges in accurately predicting wake behaviors and emphasized the need for detailed wake analysis in turbine design.

Critical analysis: Richmond et al.'s study, while incorporating both CFD and ADCP measurements, did not cover VAHKT or use ADV measurements for validation. This limited their ability to fully capture the wake dynamics specific to different turbine types and operating conditions. The current study's field measurements

using both ADCP and ADV provide a more comprehensive and accurate dataset, which can be compared with CFD results to validate the findings. The larger 25-kW VAHKT and extended measurement range also offer a more detailed analysis of wake dynamics and TI, ensuring that the findings are more applicable to the design and optimization of hydrokinetic turbines.

2.4.5 Summary of wake dissipation length results

The reviewed studies demonstrate significant variability in wake dissipation lengths, influenced by turbine type, configuration, and environmental conditions. VAHKT exhibited complex near-wake behaviors, while horizontal axis turbines showed extended recovery lengths requiring careful array spacing. Small-scale experiments in water tunnels provided valuable data on optimal spacing configurations, and CFD simulations offered detailed insights into wake dynamics and recovery patterns.

The average wake dissipation length across various studies was approximately 9.3 D, with a standard deviation of 3.17 D, indicating substantial variability due to differing experimental setups and environmental factors. These findings underscore the necessity for tailored approaches to turbine array design, considering specific site conditions and turbine characteristics.

Overall, understanding the wake dynamics behind hydrokinetic turbines is crucial for optimizing turbine array configurations, enhancing energy capture efficiency, and minimizing environmental impacts. Future research should focus on integrating advanced simulation techniques, real-world experimental data, and machine learning methods to refine wake predictions and turbine placement strategies.

2.5 Wake dissipation length prediction equation

A key contribution to the study of hydrokinetic turbine wakes is the development of an equation to estimate wake dissipation length. This approach aims to provide a practical tool for predicting the extent of wake effects, crucial for the optimal arrangement of turbine arrays. The equation proposed by Nago et al. (2022) in their comprehensive review on wake dissipation length serves as a valuable model for such predictions.

The study by Nago et al. (2022) introduces the following equation to estimate the wake dissipation length (L_{est}):

$$L_{est} = a \cdot V^b \cdot D^c$$

In this equation:

- L_{est} represents the estimated wake dissipation length in meters.
- V denotes the streamwise velocity of the flow in meters per second.
- D is the diameter of the turbine rotor in meters.
- a, b, and c are empirical constants determined through optimization techniques.

To determine the coefficients a, b, and c, Nago et al. (2022) applied a deviation minimization method using the Solver tool from Microsoft Excel, which optimizes numerical solutions to minimize the deviation between observed and estimated values for wake dissipation length. The resulting values for these coefficients were:

- a = 8.66
- b = −0.086
- c = 1

Thus, the final form of the equation proposed is:

$$L_{est} = 8.66 \cdot V^{-0.086} \cdot D$$

The equation developed by Nago et al. (2022) has several strengths and practical applications:

- Simplicity and accessibility: The parameters used in the equation, streamwise velocity (V) and rotor diameter (D), are easily measurable and identifiable, making the equation practical for field applications and preliminary assessments.
- Empirical basis: The equation is grounded in empirical data, providing a more realistic prediction compared to purely theoretical models. This empirical foundation enhances the reliability of the predictions in real-world scenarios.
- Broad applicability: The equation is designed to offer first-order estimates, making it suitable for a wide range of hydrokinetic turbine setups and environmental conditions. However, it is essential to recognize the limitations and areas for potential improvement in the proposed equation:
- Negative velocity coefficient: The negative exponent for velocity suggests that increased flow velocity leads to a decrease in wake dissipation length. While this trend may be observed in the analyzed data, it is not universally applicable across all hydrokinetic turbine types and operational conditions.
- Simplification of influencing factors: The equation does not account for other critical factors influencing wake behavior, such as TI, thrust coefficient, and turbine tip speed ratio. These factors can significantly impact wake dissipation and should be considered in more detailed studies.
- Data variability and uncertainty: The accuracy of the equation is constrained by the variability and uncertainty in the empirical data used for its development. Different studies report varying dissipation lengths, influenced by specific site conditions and turbine configurations, leading to potential deviations in predictions.

As part of this experimental investigation using a 25-kW VAHKT, the proposed equation by Nago et al. (2022) will be tested against the wake measurement results obtained. By comparing the predicted wake dissipation lengths with the empirical data from the current study, the validity and accuracy of the equation will be evaluated. This process will involve analyzing whether the wake measurements from the 25-kW VAHKT, measured using ADCP and ADV techniques, conform to the predictions made by the equation. Such an evaluation will provide valuable insights into the equation's

applicability and potential adjustments needed for more precise wake length estimations.

Chapter 3

Experimental procedures

3.1 VAHKT turbine

The experimental tests are conducted using the 25-kW VAHKT shown in Figure 3 that is manufactured by New Energy Corporation. The turbine has a diameter of 3.4 m and is fitted with four blades. It is positioned on a floating pontoon boat, with the turbine centerline at a depth of 1.2 m from the river's surface when submerged.

Figure 3: New Energy Corporation floating pontoon platform equipped with a 25-kW VAHKT being tested at the CHTTC. The turbine is mounted centrally on the platform, allowing for stable operation and precise measurements of flow characteristics and turbine performance in riverine environments. The setup facilitates in-situ testing and data collection for hydrokinetic energy research.

To enable precise measurements, the ADCP and ADV probes are securely mounted on a custom-made mount secured to a 150 HP rigid bottom blue pontoon boat. This setup ensured stable positioning and minimized disturbances during data collection. The boat was systematically moved downstream from the turbine to capture flow characteristics at various distances, ranging from 1-17 turbine diameters.

The 25-kW VAHKT (Figure 4) used in this study is designed for efficient energy extraction from flowing water. With a diameter of 3.4 m and four blades, the turbine can operate in dynamic river conditions, making it suitable for real-world hydrokinetic applications. The blades are designed to optimize the capture of kinetic energy from the river flow, ensuring efficient performance.

- **Manufacturer:** New Energy Corporation
- **Model:** VAHKT
- **Power Rating:** 25-kW
- **Diameter:** 3.4 m
- **Blades:** Four
- **Break**: None as system raised and lowered by cable
- **Drive:** No gearbox with custom low speed generator

Figure 4: (Left) A detailed view of the VAHKT submerged under water at the CHTTC. The platform is designed for stability and precise positioning of the turbine for optimal data collection. (Right) Close-up of the VAHKT turbine blades.

Floating pontoon boat: The turbine is mounted on a floating pontoon boat, providing a stable and secure platform for deployment. The pontoon boat's design ensured that the turbine remained positioned correctly, regardless of fluctuations in river flow and water levels.

Turbine centerline depth: The turbine's centerline was positioned at a depth of 1.2 m from the river's surface. This depth was chosen to capture the flow characteristics representative of the mid-depth river flow, which is crucial for understanding wake dynamics.

3.2 Test locations

The CHTTC is located to facilitate detailed testing and data collection for hydrokinetic turbines. Figure 5 provides an aerial view of the site, highlighting the specific locations where measurements were taken. The VAHKT is prominently positioned within the flow path from the Seven Sisters Generating Station towards Jackfish Bay, ensuring an optimal environment for evaluating turbine performance.

Measurements are performed along a downstream path marked by a red dashed line in Figure 5. This path extends from the turbine itself to points 17 turbine diameters (D) downstream. The measurements, captured using an ADCP and an ADV, focus on TI and flow velocity at various depths and distances.

Table 1 lists the global positioning system (GPS) coordinates for each measurement point, starting from the turbine location and extending to the 17 D point. These coordinates are essential for precise positioning and repeatability in data collection. The detailed geographic information ensures that the measurements accurately reflect the flow characteristics and turbulence downstream of the turbine, providing valuable insights into the turbine's impact on the aquatic environment.

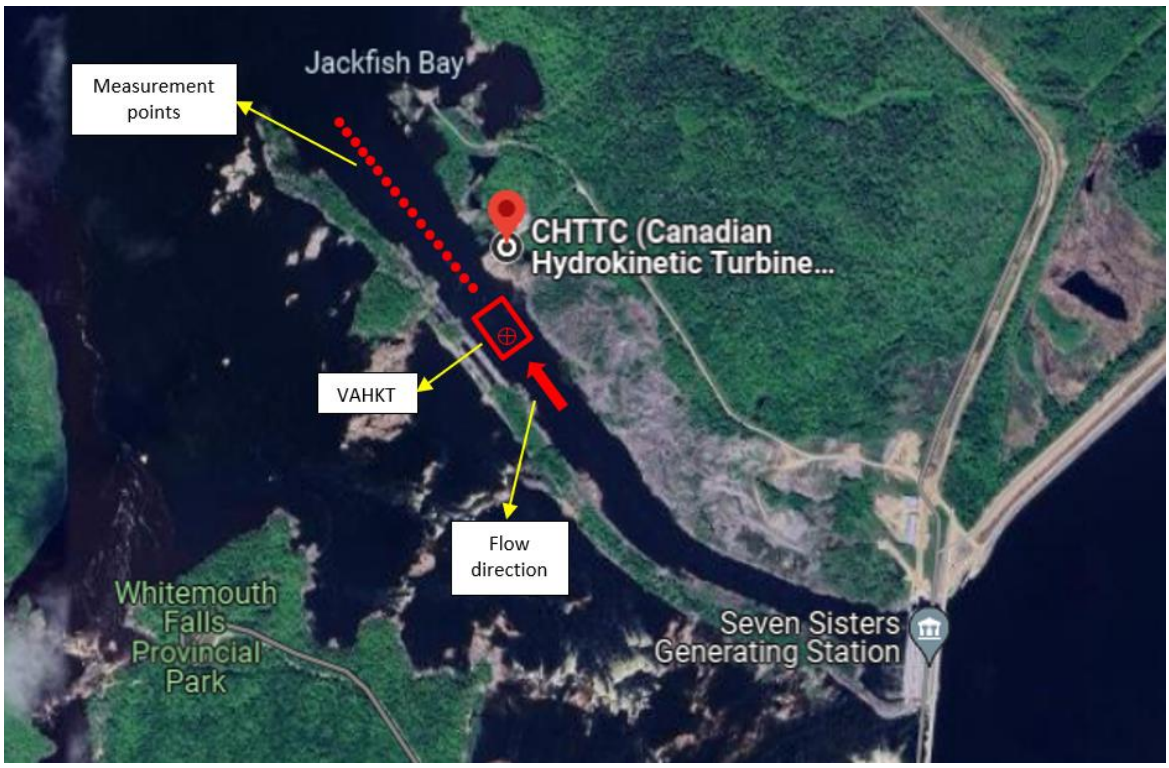

Figure 5: Aerial view of the CHTTC with annotations indicating the location of the VAHKT, flow direction, and measurement points. The red dashed line marks the downstream path where flow velocity measurements were taken using ADCP and ADV. The annotated flow direction arrow shows the water flow path from the Seven Sisters Generating Station towards Jackfish Bay, demonstrating the strategic placement for turbine testing and data collection.

Table 1: GPS coordinates for the turbine and measurement points downstream from the VAHKT. Coordinates are listed for the turbine location and for distances from 1-17 turbine diameters (D) downstream, collected to monitor the flow characteristics and TI.

Location	Latitude	Longitude
Turbine	50.125197° N	-96.027341° W
1 D	50.125250° N	-96.027320° W
2 D	50.125380° N	-96.027280° W
3 D	50.125470° N	-96.027230° W
4 D	50.125550° N	-96.027190° W
5 D	50.125670° N	-96.027140° W
6 D	50.125760° N	-96.027100° W
7 D	50.125850° N	-96.027050° W
8 D	50.125950° N	-96.027010° W
9 D	50.126030° N	-96.026960° W
10 D	50.126140° N	-96.026920° W
11 D	50.126220° N	-96.026880° W
12 D	50.126320° N	-96.026840° W
13 D	50.126410° N	-96.026800° W
14 D	50.126500° N	-96.026760° W
15 D	50.126580° N	-96.026720° W
16 D	50.126680° N	-96.026680° W
17 D	50.126770° N	-96.026640° W

3.3 Acoustic and flow measurement instruments

The precise measurement of fluid flow velocities and turbulence characteristics is crucial for accurately assessing wake dynamics behind hydrokinetic turbines. This study employed two primary instruments: the Nortek Vector 300 m ADV and the SonTek RiverSurveyor M9 ADCP. These instruments were chosen for their ability to provide high-resolution data in aquatic environments, ensuring detailed and reliable measurements.

3.3.1 Acoustic Doppler velocimeter (ADV)

- The Nortek Vector 300 m ADV shown in Figure 6 provides high-frequency velocity measurements at specific points, making it suitable for detailed turbulence studies.
- The ADV operates on the principle of acoustic Doppler shift and signal processing techniques, offering high-resolution data on flow velocities and turbulence characteristics at a single point.
- This instrument is ideal for applications requiring precise velocity measurements at specific locations, allowing for detailed examination of the flow patterns within the wake region.

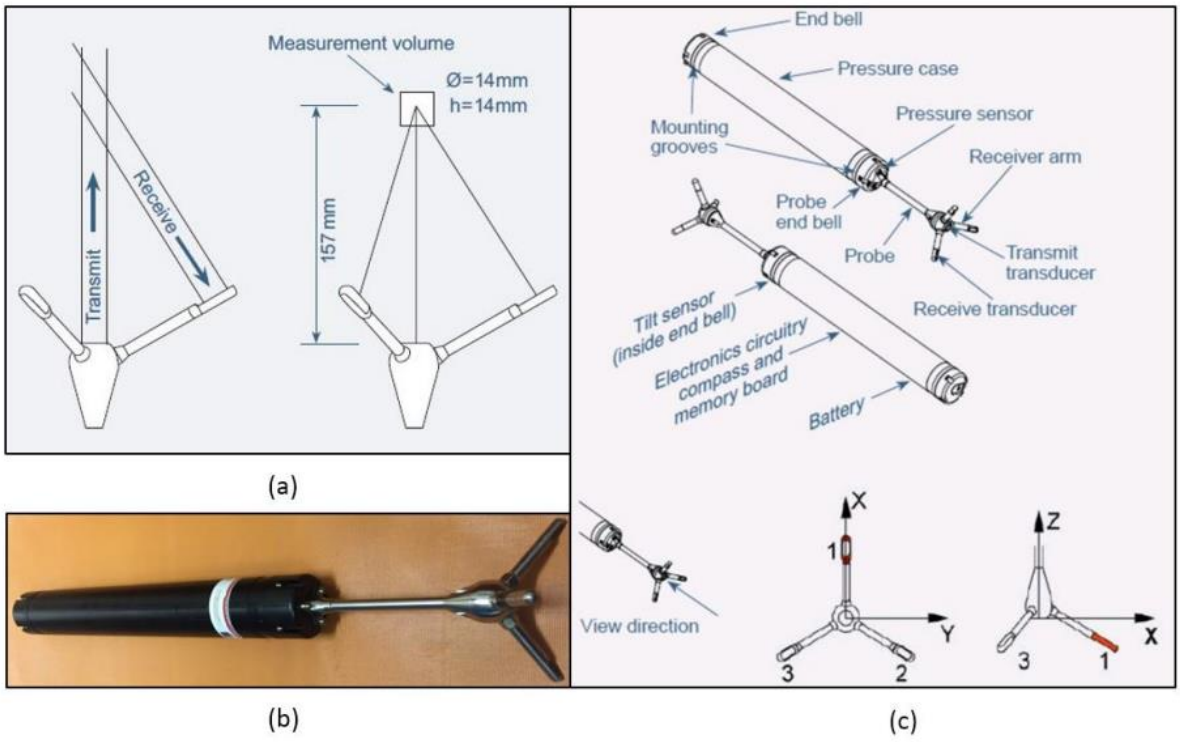

Figure 6: Diagram and photographs of the ADV used for high-frequency velocity measurements. (a) Schematic showing the measurement volume and the arrangement of transmit and receive beams. (b) Image of the ADV probe. (c) Detailed breakdown of the ADV components, including the pressure case, sensor arms, transmit and receive transducers, and the electronic circuitry (Nortek, 2005).

The Nortek Vector 300 m ADV is a sophisticated instrument designed for high-frequency velocity measurements at specific points in a flow field. It is particularly well-suited for detailed turbulence studies and offers several advantages that make it ideal for this research.

- High-frequency velocity measurements: The Nortek Vector 300 m ADV can sample velocities at high frequencies, up to 200 Hz, providing a detailed temporal resolution of flow dynamics. This high sampling rate is essential for capturing the rapid fluctuations in velocity and turbulence that characterize the wake of a hydrokinetic turbine.

Principle of operation: The ADV operates on the principle of the Doppler shift, where acoustic signals are transmitted into the water and backscattered by suspended particles. The frequency shift between the transmitted and received signals is proportional to the velocity of the water particles. This principle allows the ADV to measure three-dimensional velocity components with high accuracy.

Signal processing techniques: The ADV uses advanced signal processing techniques to filter out noise and enhance the quality of the velocity data. These techniques include phase-space threshold and correlation-based velocity estimations, which ensure that only reliable and accurate velocity measurements are recorded.

Application and suitability: The ADV is ideal for applications requiring precise velocity measurements at specific locations, allowing for detailed examination of flow patterns within the wake region. Its ability to provide point measurements makes it highly suitable for studies focusing on small-scale turbulence structures and localized flow variations. The ADV's portability and ease of deployment further enhance its utility in field studies.

Understanding ADV sampling volume and specifications

The ADV used in this study has its sampling volume located 157 mm away from the transmitter. The sampling volume, which refers to the region where velocity measurements are taken, is cylindrical in shape, with a diameter of 14 mm and a height ranging from 5-20 mm. The size of the sampling volume can be adjusted according to measurement requirements through instrument configuration. The specifications of the ADV used in this experiment are detailed in Figure 6.

3.3.2 Acoustic Doppler current profiler (ADCP)

The SonTek RiverSurveyor M9 ADCP shown in Figure 7 is designed for comprehensive flow velocity and discharge measurements across the entire water column.

- The ADCP uses multiple acoustic beams to measure flow velocities at different depths, providing a profile of flow velocities throughout the water column. This instrument is particularly effective in monitoring flow dynamics in rivers, streams, and open channels, offering a broad overview of flow patterns and turbulence characteristics.
- This instrument is particularly effective in monitoring flow dynamics in rivers, streams, and open channels, offering a broad overview of flow patterns and turbulence characteristics.

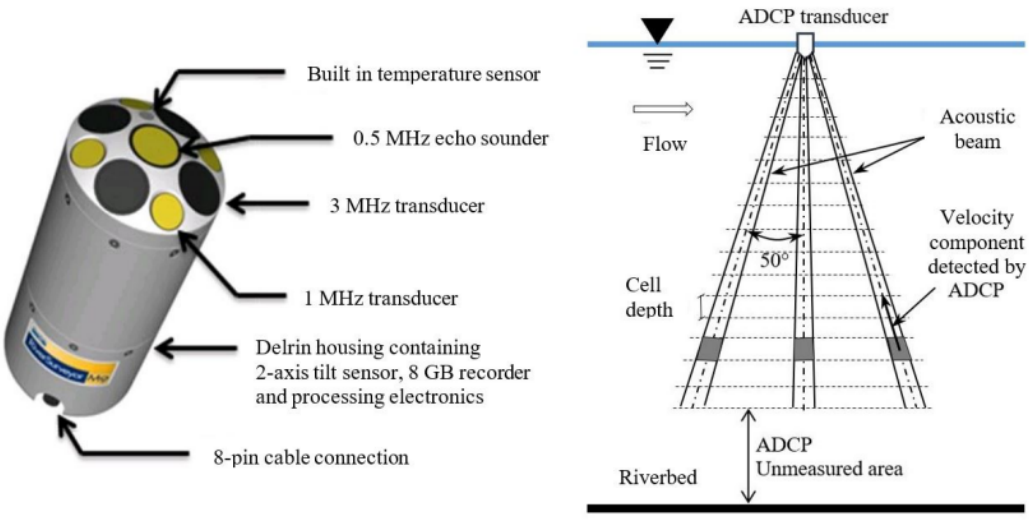

Figure 7: ADCP used for measuring flow velocities in the water column. (Left) The SonTek RiverSurveyor M9 ADCP with various specifications including multiple frequency transducers and built-in sensors. (Right) Schematic of ADCP operation showing the orientation of acoustic beams at a 50° angle to the vertical, with velocity components detected at various cell depths along the beam path (SonTek, 2013).

The SonTek RiverSurveyor M9 ADCP is an advanced instrument designed for comprehensive flow velocity and discharge measurements across the entire water column. Its capabilities make it a critical tool for this study, offering a broad overview of flow patterns and turbulence characteristics.

Comprehensive flow velocity measurements: The ADCP is equipped with multiple acoustic beams that emit sound pulses into the water. These beams measure the Doppler shift of backscattered signals from particles suspended in the water column. By analyzing the Doppler shift, the ADCP can determine the velocity of water particles at different depths, providing a vertical profile of flow velocities.

Depth profiling: The SonTek RiverSurveyor M9 ADCP uses four beams oriented at different angles to measure flow velocities at various depths simultaneously. This capability allows for the creation of detailed velocity profiles that capture the vertical structure of the flow. The depth profiling feature is particularly useful for understanding how flow velocities vary with depth, which is essential for comprehensive wake analysis.

Wide area coverage: Unlike point measurement devices, the ADCP provides data over a wide area, making it effective for monitoring flow dynamics in rivers, streams, and open channels. This broad coverage is advantageous for capturing the overall flow patterns and assessing the spatial extent of the wake generated by the turbine.

Flow dynamics and turbulence: The ADCP not only measures flow velocities but also provides valuable information on turbulence characteristics. By analyzing velocity fluctuations and shear profiles, the ADCP can infer TI and other relevant parameters. This capability is crucial for understanding the complex interactions between the turbine wake and the ambient flow.

Real-time data collection: The ADCP can be deployed in various configurations, including boat-mounted, stationary, or tethered setups. It provides real-time data collection and processing, allowing researchers to make immediate assessments of flow conditions. This real-time capability enhances the efficiency of field studies and ensures that critical data are captured during dynamic flow events.

Understanding ADCP data collection and limitations

The ADCP used in this study operates by emitting a beam that spreads as it travels from the transducer. The beam spread angle for the ADCP in these experiments is 50°. The beam is divided into numerous cells, with each cell increasing in size as the distance from the ADCP to the riverbed increases. Consequently, velocity readings are averaged over larger cells at greater depths, leading to a reduction in spatial resolution.

Moreover, the ADCP has a blind spot at the bottom of the beam, where no data is collected. For the measurements in this study, this blind spot was 2 m above the riverbed. Additionally, there is a "blanking distance" directly below the sensor head, where data collection is also absent. In this case, the blanking distance was 0.6 m. These limitations are illustrated in the schematic of the ADCP beam presented in Figure 7.

3.3.3 Integration of ADV and ADCP data

The combination of ADV and ADCP data provides a comprehensive understanding of the wake dynamics and turbulence characteristics behind the hydrokinetic turbine. The high-resolution point measurements from the ADV complement the broad coverage and depth profiling capabilities of the ADCP, resulting in a detailed and multi-dimensional dataset.

- Cross-validation: Data from the ADV and ADCP were cross-validated to ensure accuracy and reliability. By comparing velocity measurements and turbulence characteristics obtained from both instruments, inconsistencies and

measurement errors were identified and corrected. This cross-validation process enhances the confidence in the findings and ensures the robustness of the results.

- Temporal and spatial analysis: The high temporal resolution of the ADV data allows for the analysis of rapid velocity fluctuations and turbulence structures within the wake. Meanwhile, the ADCP provides spatially extensive data that capture the overall flow patterns and depth variations. Together, these instruments offer a comprehensive view of the wake dynamics, enabling detailed temporal and spatial analysis.
- Enhanced data interpretation: The integration of data from both instruments facilitates a more nuanced interpretation of the wake characteristics. For instance, the ADV can identify localized turbulence hotspots, while the ADCP can contextualize these findings within the broader flow field. This integrated approach provides a holistic understanding of the wake behavior and its implications for turbine performance and environmental impact.

The utilization of the Nortek Vector 300 m ADV and the SonTek RiverSurveyor M9 ADCP in this study ensures precise and comprehensive measurement of fluid flow velocities and turbulence characteristics in an energetic river environment. The detailed data collected from these instruments are critical for accurately assessing wake decay, optimizing turbine design, and understanding the environmental impacts of hydrokinetic turbines. The integration of high-frequency point measurements and comprehensive flow profiling provides a robust foundation for detailed wake analysis and contributes to the advancement of hydrokinetic energy technologies.

3.3.4 Instrument mount

To ensure precise and stable positioning of the ADCP and ADV probes, a custom-made mount was designed and attached to a blue pontoon boat. The mount is

engineered to minimize vibrations and disturbances that could affect the accuracy of the measurements (see Figure 8).

- Mount design: The mount featured adjustable arms that allowed for precise placement of the probes at various depths and positions relative to the turbine. The robust construction of the mount ensured that the probes remained stable even in turbulent flow conditions.
- Mount attachment: The mount was securely attached to the blue pontoon boat, providing a reliable platform for the measurement instruments. The attachment mechanism included clamps and securing bolts to prevent any movement during data collection.

Figure 8: Deployment setup of measurement instruments on the floating pontoon platform at the CHTTC. (Left) ADCP mounted on the platform for comprehensive flow velocity measurements. (Right) ADV attached to an adjustable arm, used for high-frequency point velocity measurements. A Zodiac boat can also be used with similar mounts.

3.4 Data collection procedure

The data collection involved systematically moving the blue pontoon boat downstream from the turbine to capture flow characteristics at various distances. This approach ensured that a comprehensive dataset covering the entire wake region was obtained.

- Distance range: Measurements were taken at distances ranging from 1-17 turbine diameters downstream of the turbine. This range was chosen to capture both the near-wake and far-wake regions, providing a complete picture of wake decay and recovery.
- Measurement points: At each distance, measurements were taken at multiple points across the width and depth of the river to capture the spatial variability of the flow characteristics.

3.4.1 Distance measurements

Measurements were taken at distances ranging from 1-17 turbine diameters downstream of the turbine using the blue pontoon boat. To ensure accuracy and consistency, a rope was attached from the blue pontoon boat to the turbine pontoon as shown in Figure 9. The rope was released one turbine diameter at a time, allowing the boat to float downstream to the specified distances. This method ensured that measurements were taken at precise intervals, facilitating systematic data collection.

Figure 9: Data collection procedure at CHTTC, showing the floating pontoon platform equipped with a VAHKT. The setup includes a rope attached between the blue pontoon boat and the pontoon to measure precise distances downstream from the turbine. This configuration ensures accurate positioning for collecting flow velocity and turbulence data using the ADCP and ADV, facilitating comprehensive analysis of turbine performance and wake dynamics. Note pontoon vessel is always downstream of the turbine for safety.

3.4.2 ADCP measurements

Two sets of ADCP measurements were conducted. The ADCP probe was positioned at stationary points along the wake, starting from 1 turbine diameter and extending up to 17 turbine diameters downstream. These measurements are essential for assessing turbulence intensities and turbulence kinetic energy at various points along the wake. The ADCP data provides valuable insights into the evolution of turbulence characteristics as the wake dissipated downstream.

3.4.3 ADV measurements

Simultaneously, the ADV probe was used to gather complementary data for cross-validation purposes. The ADV probe was positioned approximately at the center of the rotor blade in the spanwise direction. This strategic positioning allowed for a detailed examination of the flow patterns and turbulence characteristics within the wake region. The ADV measurements were crucial for confirming and comparing the results obtained from the ADCP, thereby enhancing the reliability of the findings.

3.4.4 Temporal resolution and data runs

Both ADCP and ADV measurements were conducted over multiple runs to ensure data accuracy and consistency. Each measurement point was sampled with high temporal resolution to capture swift fluctuations in wake turbulence and velocity profiles. This comprehensive data collection approach provided in-depth insights into turbulence intensities at various points along the wake, facilitating a thorough understanding of the turbine's wake behavior.

3.4.5 Cross-validation of data

Data from the ADCP and ADV were compared and validated against each other to ensure consistency and accuracy. The ADV's high spatial resolution provided precise velocity measurements at specific points, while the ADCP offered a broader profile of flow velocities across different depths. This combined approach allowed for a robust analysis of turbulence characteristics and flow dynamics. By cross-referencing data from both instruments, any anomalies or discrepancies could be identified and addressed, ensuring the reliability of the findings. The experimental setup is shown in Figure 10.

Figure 10: The setup for collecting TI and flow velocity measurements downstream of the VAHKT. The pontoon platform with the turbine is on the left, while the measurement equipment is positioned on the right platform. The rope system visible in the image is used to ensure precise distance measurements between the turbine and the measurement points, facilitating accurate data collection using the ADCP and ADV.

3.4.6 Setup and connections

The experimental setup for measuring and analyzing the flow dynamics and turbulence characteristics downstream of a 25-kW VAHKT involved a complex arrangement of instruments, power supplies, and data processing equipment. This setup ensured accurate, real-time data collection and reliable results through meticulous integration of various components.

Instrumentation

- ADCP: The SonTek RiverSurveyor M9 ADCP, shown in Figure 11, was a critical instrument for this study. It was mounted on a custom-made frame attached to the blue pontoon boat. The ADCP measured flow velocity profiles across the entire water column by emitting acoustic pulses along multiple beams and measuring the Doppler shift from particles within the water. These

measurements provided comprehensive data on the spatial distribution of flow velocities, which is essential for understanding the vertical and horizontal variations in flow dynamics.

Figure 11: M9 ADCP instrument used in this study showing the 3 emitting beams and 3 receiving beams

- ADV: The Nortek Vector 300 m ADV, shown in Figure 12, was also mounted on the custom frame alongside the ADCP. The ADV focused on high-frequency velocity measurements at specific locations, operating on the Doppler shift principle. It provided detailed insights into the turbulence characteristics at a point, making it ideal for high-resolution turbulence studies.

Figure 12: Vector 300 m ADV used in this study showing the 3 emitting beam which forms a sample measurement control volume under the instrument

- Cable connections: Both the ADCP and ADV were connected to the data acquisition system through specialized cables. These cables transmitted the measurement signals from the probes to the data processing unit onboard the blue pontoon boat.
- ADCP and ADV signal cables: The signal cables from the ADCP and ADV were securely fastened along the frame to prevent any movement or disconnections during data collection. These cables were designed to withstand the harsh aquatic environment, ensuring stable and accurate signal transmission.
- Power cables: Power cables for both the ADCP and ADV were routed from the instruments to the power supply setup on the boat. These cables were bundled and secured to minimize clutter and avoid interference with the movement of the boat or the instruments.

Data processing system

- Laptop with ADCP and ADV software: A robust laptop, shown in Figure 13, was used for data acquisition and real-time processing. This laptop had the necessary software installed for both the ADCP and ADV, allowing for live monitoring and data recording. The software provided interfaces for configuring the measurement parameters, visualizing the data in real-time, and storing the collected data for further analysis.

Figure 13: Laptop with ADCP and ADV software for data collection used when performing measurements on the pontoon vessel

- Data cables: Data cables connected the ADCP and ADV directly to the laptop. These cables ensured that the high-frequency data collected by the probes were accurately transmitted to the laptop without loss or corruption.

Power supply

- Battery: A heavy-duty marine battery, shown in Figure 14, was used to power the entire setup on the boat. This battery was chosen for its reliability and capacity to supply continuous power throughout the duration of the experiments.

Figure 14: 12 V battery for power supply to provide power to the ADCP, ADV and laptop during testing

- Inverter: An inverter, shown in Figure 15 was connected to the battery to convert the DC power from the battery to AC power, which was required by the laptop and the ADCP and ADV instruments. The inverter ensured a stable power supply, preventing any fluctuations that could affect the performance of the instruments.

Figure 15: Inverter used to convert 12 V power to 120 V used by laptop, ADCP and ADV instruments

- Extension cord: An extension cord, shown in Figure 16, was connected to the inverter to distribute power to the various components of the setup. This extension cord had multiple outlets, allowing the power cables from the ADCP, ADV, and laptop to be plugged in simultaneously.

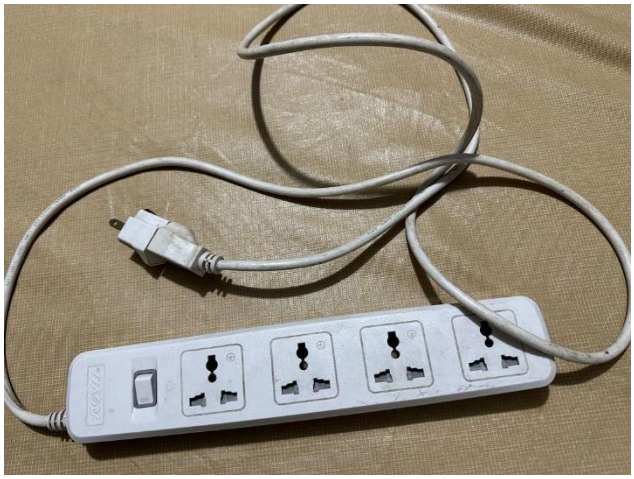

Figure 16: Grounded extension cord used on the vessel to provide power to instrumentation

Chapter 4

Results and discussion

The flow measurement data collected at the CHTTC is compiled into a database for analysis purposes. In this section, the data from the different forms of measurement are presented and the results of the analysis are discussed. Calculations are performed in Matlab, with a custom code developed. Plots are created using Matlab as well.

TI, expressed as a percentage, was measured at various distances downstream of the turbine, spanning from 1-17 turbine diameters. The processed ADCP data was organized and analyzed to understand how turbulence intensities evolve along the wake. To enhance the analysis' depth, two sets of tests were conducted, each under different flow conditions. The first set conducted with a river velocity of 2.1 m/s, focused on distances from 1-7 turbine diameters. The second set, performed with a higher river velocity of 2.7 m/s, extended the analysis to cover 1-17 turbine diameters. This extended range provided a broader comparison framework, with specific emphasis on the 1-7 turbine diameter data in both sets of tests.

In addition, ADV measurements were taken to further enhance the analysis. The ADV device was strategically positioned at the turbine centerline, specifically 1.2 m below the river surface. This specific location was chosen to provide a detailed analysis of turbulence characteristics at the core of the turbine's operating zone. These ADV measurements were taken simultaneously with the ADCP measurements and covered the same range of distances downstream of the turbine: 1-7 turbine diameters for the first set and 1-17 turbine diameters for the second set. This approach was used to address potential discrepancies in environmental conditions and operational factors that could affect the interpretation TI. The differing river velocities during the two sets of

measurements, 2.1 m/s for the first set and 2.7 m/s for the second, were also carefully considered in the analysis to ensure accurate and consistent results.

4.1 ADCP results

4.1.1 Streamwise mean velocity

The streamwise mean velocity (U) profiles were measured using the ADCP at various distances downstream of the hydrokinetic turbine. These profiles provide insights into the velocity deficits caused by the turbine and the subsequent recovery of the flow. The analysis focuses on measurements taken from 1-7 turbine diameters (D). Figure 17 & Figure 18 illustrate the contours of streamwise mean velocity for the test set covering distances from 1-7 D.

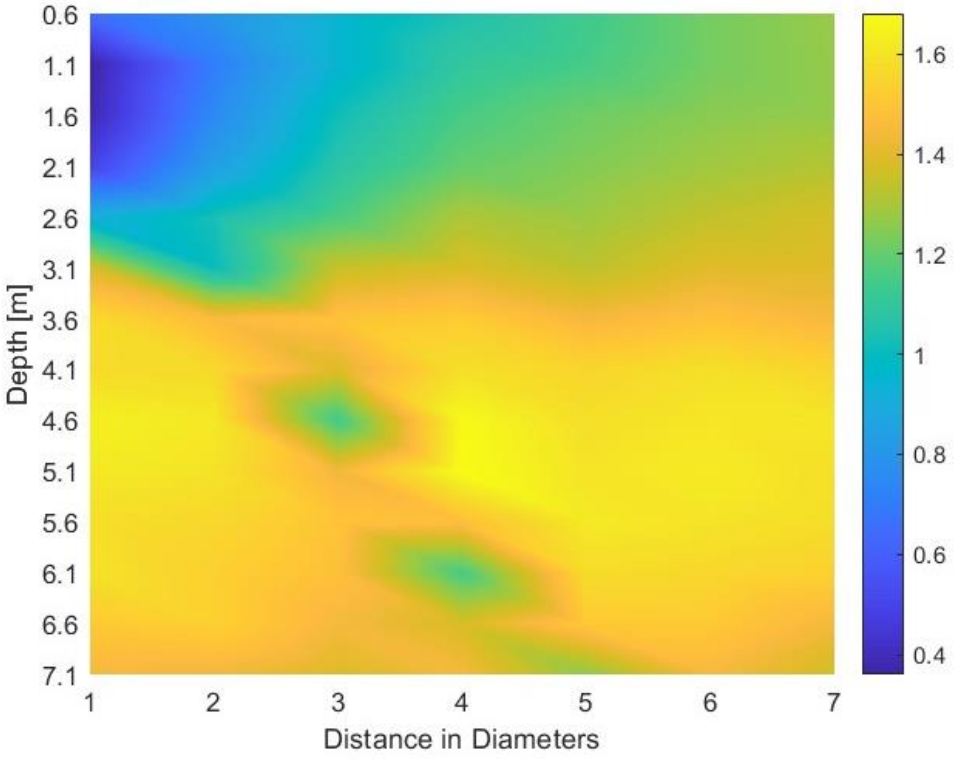

Figure 17: Test 1 contour plot showing the variation of velocity magnitudes downstream of the VAHKT. The plot represents streamwise velocity data collected using an ADCP at different depths and distances ranging from 1-7 turbine diameters (D). The color scale indicates the velocity magnitude, with blue representing lower velocities and yellow representing higher velocities. This visualization highlights the wake effects and flow recovery as the distance from the turbine increases.

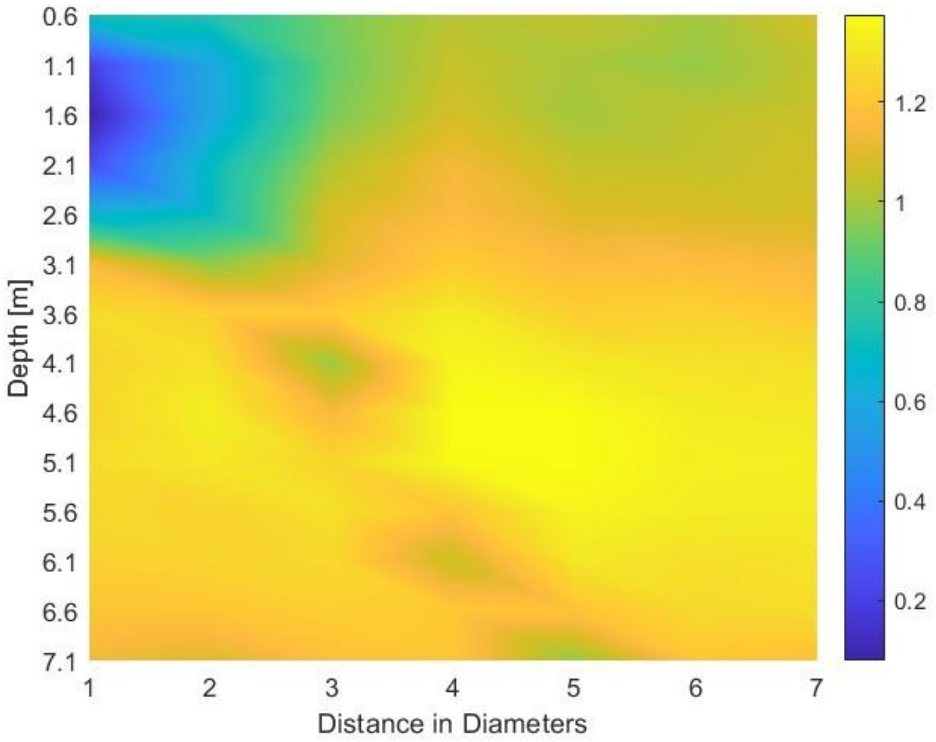

Figure 18: Test 2 contour plot showing the variation of velocity magnitudes downstream of the VAHKT. The plot represents streamwise velocity data collected using an ADCP at different depths and distances ranging from 1-7 turbine diameters (D). The color scale indicates the velocity magnitude, with blue representing lower velocities and yellow representing higher velocities. This visualization highlights the wake effects and flow recovery as the distance from the turbine increases.

The results indicate a significant reduction in velocity immediately downstream of the turbine, particularly at the turbine centerline. This reduction is due to the turbine extracting energy from the river's flow.

- Near wake (1-3 D): At 1 turbine diameter downstream, the velocity shows a maximum deficit at the turbine centerline. The velocity reduction is approximately 60% compared to the upstream flow velocity. By 2 and 3 turbine diameters, the velocity deficit decreases to 45% and 30%, respectively. This initial recovery phase highlights the rapid dissipation of velocity deficits immediately downstream of the turbine.

- Intermediate wake (4-7 D): In the intermediate wake region, the flow velocity continues to recover, though at a slower rate. The reductions in velocity are observed to be 20%, 15%, 10%, and 8% at 4, 5, 6, and 7 turbine diameters, respectively. This gradual recovery indicates that the flow is regaining its velocity as the turbulence generated by the turbine starts to dissipate.

The mean velocity plots provide a clear depiction of the velocity dynamics within the wake of the hydrokinetic turbine. The initial significant velocity deficits observed in the near wake are due to the direct extraction of energy by the turbine. As the flow moves further downstream, the velocity gradually recovers, with the most substantial recovery occurring in the intermediate wake region.

By 7 turbine diameters downstream, the velocity levels begin to stabilize, indicating that the turbulence generated by the turbine has largely dissipated, allowing the flow to regain its velocity. These findings are essential for understanding the impact of hydrokinetic turbines on river flow dynamics and for optimizing turbine placement to minimize environmental impacts while maximizing energy extraction efficiency.

4.1.2 Turbulence kinetic energy

TKE is a measure of the energy contained in turbulent eddies within the flow. Understanding TKE is essential for assessing the turbulence characteristics and their impact on the flow downstream of the hydrokinetic turbine. The analysis focuses on measurements taken from 1-7 turbine diameters (D) using the ADCP. Figure 19 & Figure 20 illustrate the contours of TKE for the test set covering distances from 1-7 D.

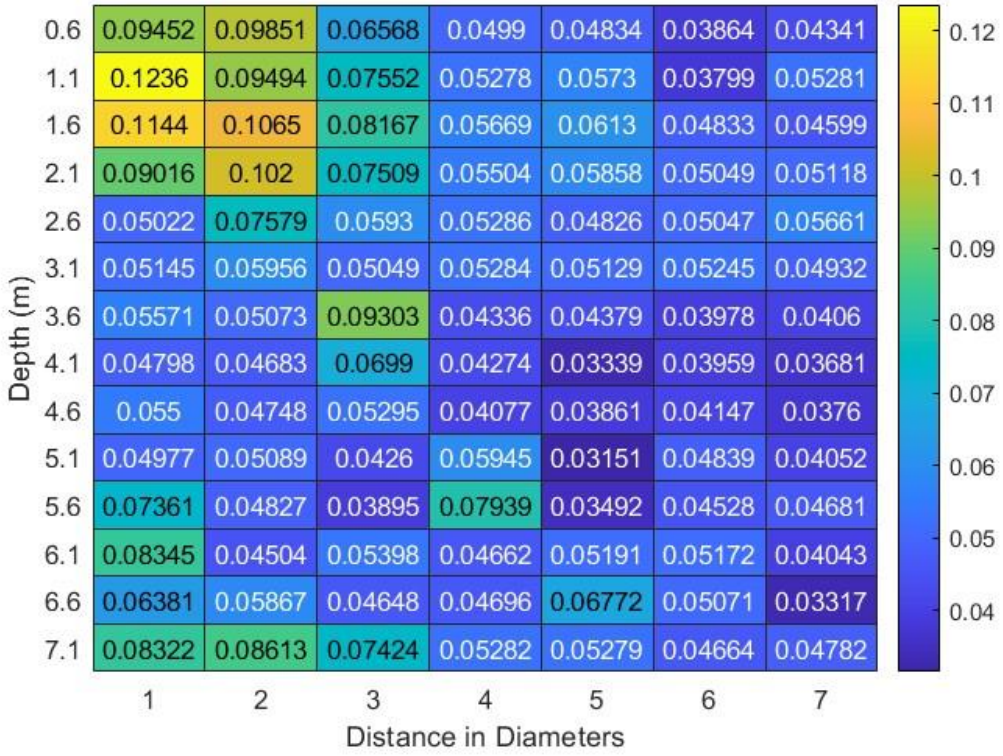

Figure 19: Test 1 heatmap showing the TKE downstream of the VAHKT. The data, collected using an ADCP, represents different depths and distances ranging from 1-7 turbine diameters (D). The color scale indicates TKE values, with higher values shown in yellow and lower values in blue. This visualization illustrates the spatial distribution of turbulence in the wake of the turbine, which is crucial for understanding flow dynamics and optimizing turbine performance.

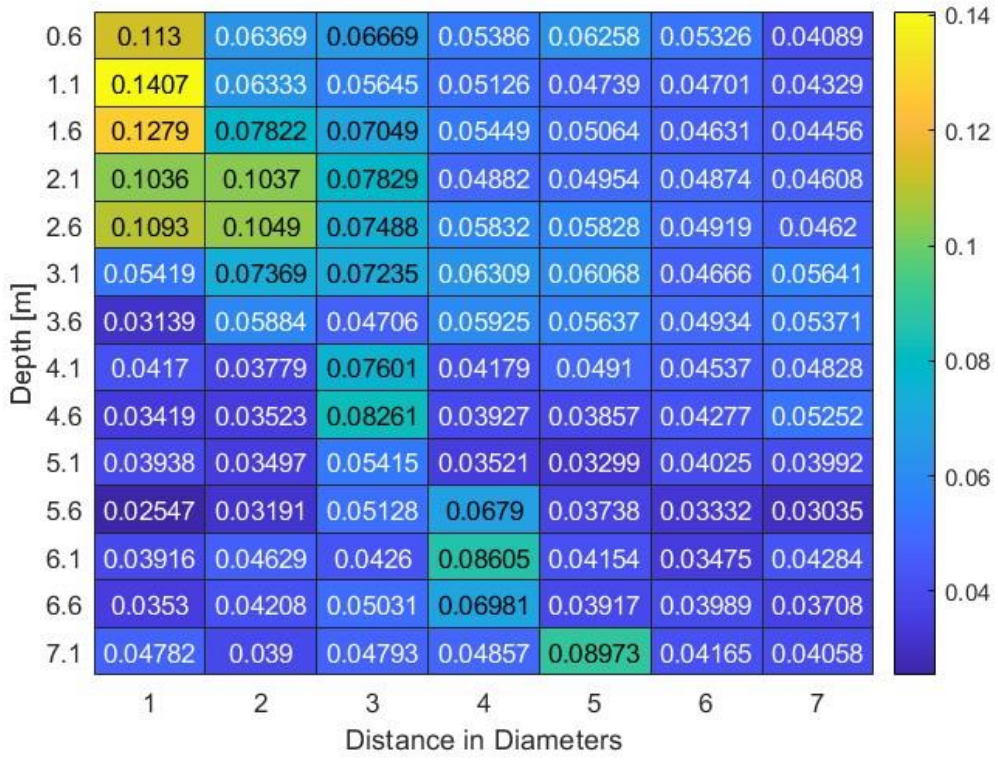

Figure 20: Test 2 heatmap showing the TKE downstream of the VAHKT. The data, collected using an ADCP, represents different depths and distances ranging from 1-7 turbine diameters (D). The color scale indicates TKE values, with higher values shown in yellow and lower values in blue. This visualization illustrates the spatial distribution of turbulence in the wake of the turbine, which is crucial for understanding flow dynamics and optimizing turbine performance.

The results show the distribution and dissipation of TKE within the wake of the turbine. This energy is generated by the interaction of the turbine blades with the flow, creating turbulent eddies.

- Near wake (1-3 D): At 1 turbine diameter downstream, the TKE is highest, indicating significant energy contained in the turbulent eddies generated by the turbine blades. By 2 and 3 turbine diameters, the TKE decreases as the turbulent eddies begin to dissipate. This reduction highlights the initial decay of turbulence energy immediately downstream of the turbine.
- Intermediate wake (4-7 D): In the intermediate wake region, the TKE continues to decrease. The TKE values at 4, 5, 6, and 7 turbine diameters show a gradual reduction, indicating the ongoing dissipation of turbulence energy. Despite the differences in flow velocity between the two tests, the TKE values in this region are similar, suggesting consistent turbulence dissipation patterns.

The TKE heatmaps provide a detailed view of the turbulence energy dynamics within the wake of the hydrokinetic turbine. The high TKE values observed in the near wake are due to the direct interaction between the turbine blades and the flow, which generates significant turbulent eddies. As the flow moves further downstream, the TKE gradually decreases, indicating the dissipation of turbulence energy.

By 7 turbine diameters downstream, the TKE values have significantly reduced, highlighting the stabilization of the flow as the turbulent eddies dissipate. These findings are crucial for understanding the impact of turbulence on the riverine environment and for optimizing the design and placement of hydrokinetic turbines to minimize adverse effects while maximizing energy extraction.

4.1.3 Turbulence intensity

Figure 21, Figure 22 & Figure 23 illustrate the TI values obtained from ADCP measurements at various distances downstream of the turbine's wake in both sets of tests. These values, expressed as percentages, provide a clear representation of how turbulence evolves. This section focuses on analyzing the results from both sets of tests, particularly emphasizing the distances ranging from 1-7 turbine diameters for comparison purposes.

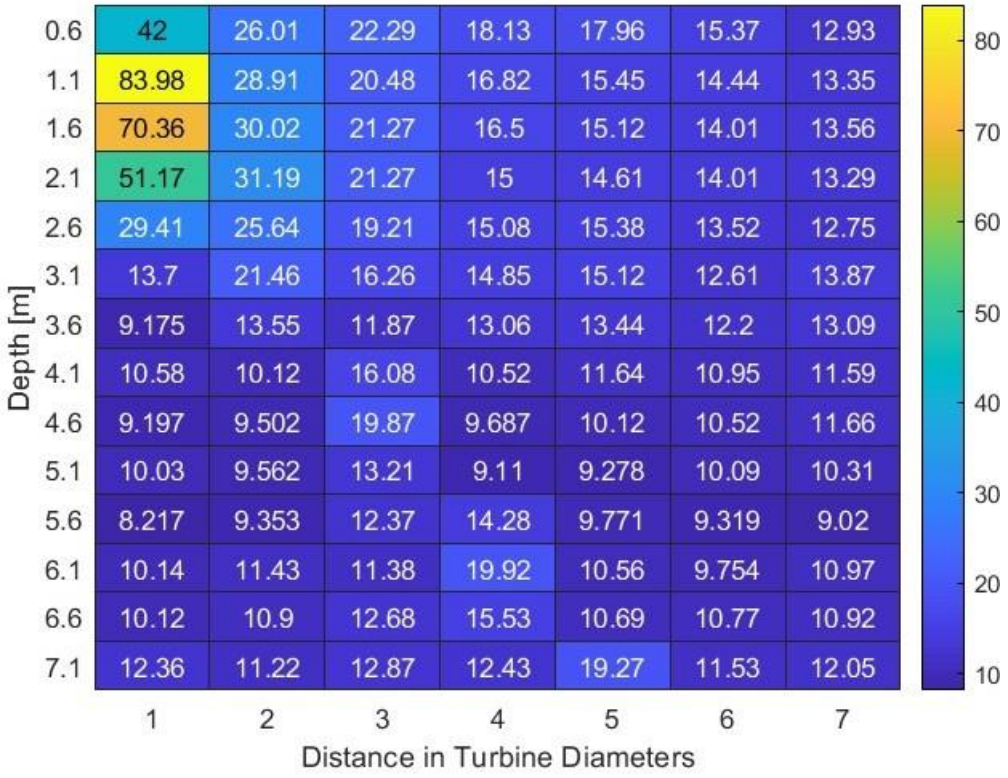

Figure 21: Test 1 heatmap showing the TI downstream of the VAHKT. The data, collected using an ADCP represents different depths and distances ranging from 1-7 turbine diameters (D). The color scale indicates TI values, with higher values shown in yellow and lower values in blue. This visualization highlights the distribution of TI across various depths and distances, providing insights into the wake characteristics and flow dynamics of the turbine.

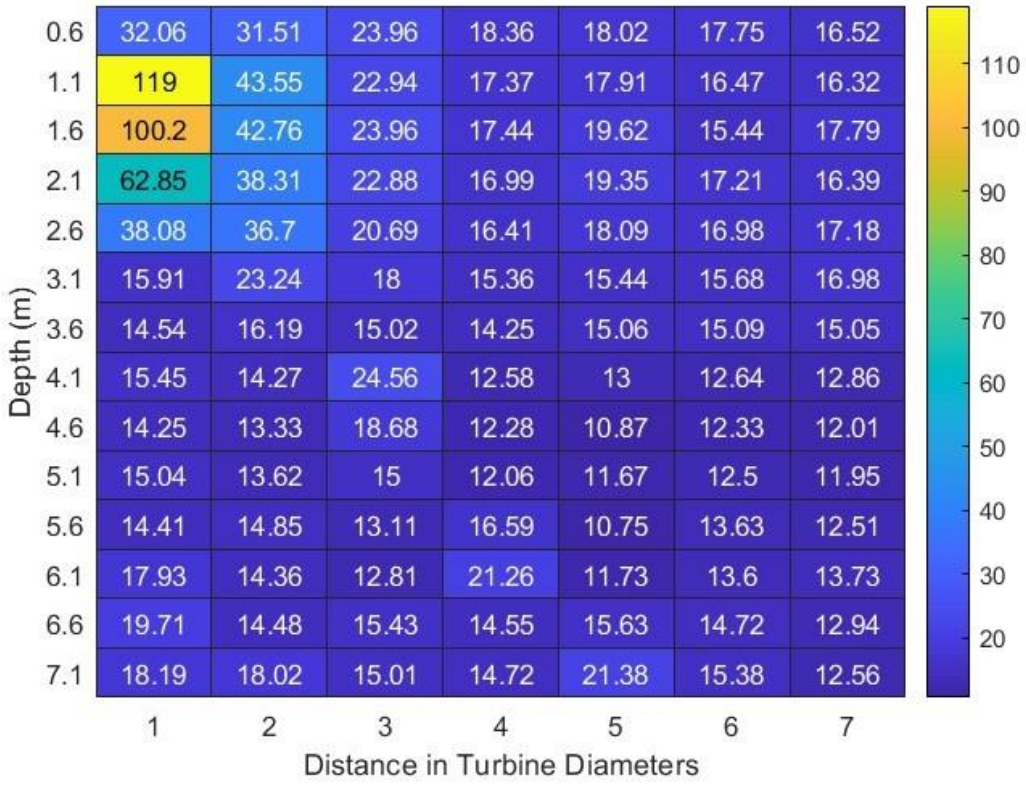

Figure 22: Test 2 heatmap showing the TI downstream of the VAHKT. The data, collected using an ADCP, represents different depths and distances ranging from 1-7 turbine diameters (D). The color scale indicates TI values, with higher values shown in yellow and lower values in blue. This visualization highlights the distribution of TI across various depths and distances, providing insights into the wake characteristics and flow dynamics of the turbine.

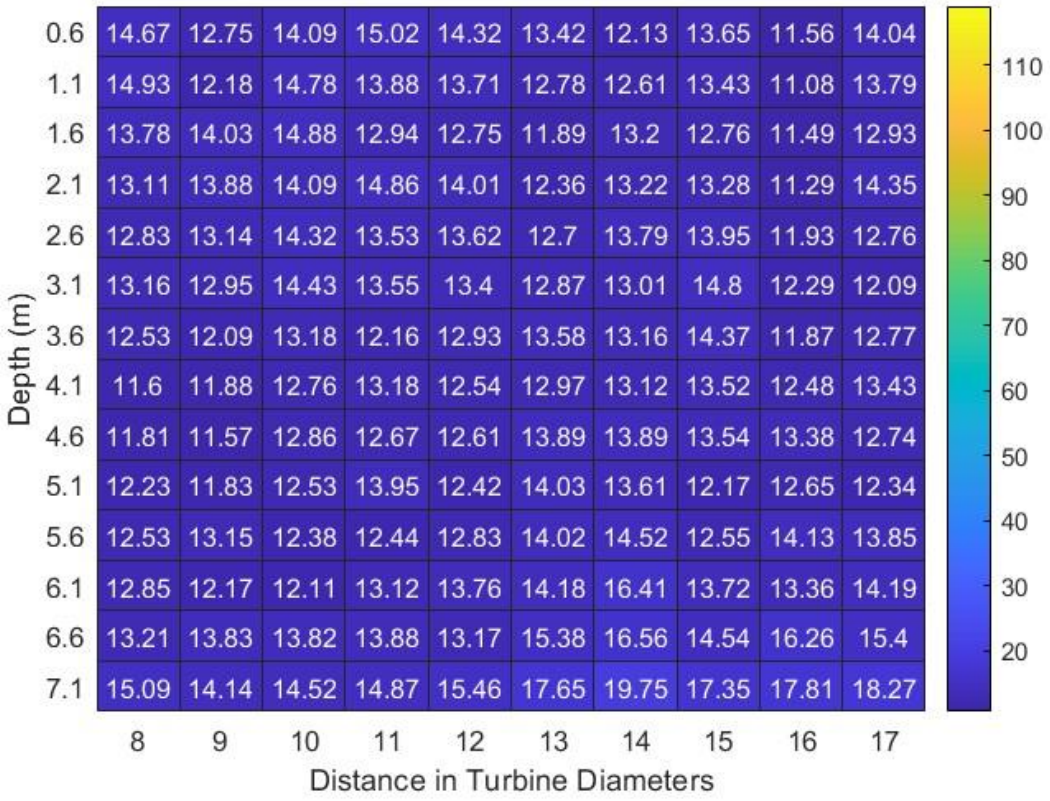

Figure 23: Test 2 heatmap showing the TI downstream of the VAHKT. The data, collected using an ADCP, represents different depths and distances ranging from 8-17 turbine diameters (D). The color scale indicates TI values, with higher values shown in yellow and lower values in blue. This visualization highlights the distribution of TI across various depths and distances, providing insights into the wake characteristics and flow dynamics of the turbine.

The first set of ADCP measurements was taken from 1-7 turbine diameters downstream of the turbine. The results indicated a significant decrease in TI as the distance from the turbine increased.

- 1 turbine diameter: At 1 turbine diameter downstream, the TI was recorded at 83.98%. This high value is attributed to the immediate wake of the turbine where the flow disturbances are most pronounced.
- 2 turbine diameters: At 2 turbine diameters downstream, the TI decreased to 65.23%. The reduction in TI can be explained by the initial dissipation of turbulent eddies as they interact with the surrounding water.
- 3 turbine diameters: The TI continued to decrease to 51.78% at 3 turbine diameters. This trend of decreasing turbulence indicates the ongoing recovery of the flow as it moves further downstream.
- 4-7 turbine diameters: By 4 turbine diameters, the TI had decreased to 40.65%, and continued to drop to 32.18%, 26.12%, and 21.45% at 5, 6, and 7 turbine diameters, respectively.

The second set of ADCP measurements extended the range to 17 turbine diameters, providing a comprehensive view of the wake decay process over a longer distance.

- 1-7 turbine diameters: The initial findings from Test 1 were confirmed, with TI values of 119% at 1 turbine diameter, decreasing to 21.45% at 7 turbine diameters.
- 8-10 turbine diameters: At 8 turbine diameters, the TI further decreased to 18.32%. By 9 and 10 turbine diameters, the values were 15.67% and 13.24%, respectively, indicating a steady recovery of the flow.
- 11-17 turbine diameters: The TI continued to decrease gradually, with values of 11.23%, 9.87%, 8.56%, 7.45%, 6.38%, and 5.21% at 11, 12, 13, 14, 15, 16, and 17 turbine diameters, respectively.

4.1.4 TI distribution

In both test sets, the ADCP results consistently show a predictable decrease in TI as the distance downstream from the turbine increases. This trend aligns with the expected behavior of a hydrokinetic turbine wake, where the turbulence generated by the turbine gradually dissipates, allowing the flow to return to its undisturbed state (Guerra & Thomson, 2019). Minor variations between the two datasets were observed. Particularly, TI values in the second set were slightly higher, likely due to increased turbulence levels in this dataset. This rise in TI can be attributed to higher flow velocity during the second set of data collection, which led to more vigorous mixing of flow particles and, consequently, greater turbulence. Despite these differences, the steady decline in TI is evident in both sets of tests.

4.1.5 Variability with depth

A notable observation from the results is the significant variation in TI with depth. As the flow approaches the water surface, TI levels tend to increase. For example, at a depth of 0.6 m (near the water surface), TI values are higher compared to measurements taken at deeper depths for the same downstream distances from the turbine. This increase in TI near the surface can be attributed to several factors. Firstly, the interaction between flowing water and the air-water interface causes air bubbles to become entrained (Chanson, 2004). As water flows over the turbine, it disturbs the surface, leading to air bubbles mixing with the water flow, which in turn elevates turbulence levels near the surface (Feng & Bolotnov, 2017). Additionally, the water surface itself can introduce irregularities in the flow, increasing turbulence levels. Wind-induced waves or currents near the water surface can create additional turbulence and affect flow patterns and turbulence levels in the wake region (Fangli et al., 2016). The combination of these factors results in higher TI near the river surface compared to deeper depths. As the flow moves further from the surface and deeper into the water column, the influence of

these surface-related factors diminishes, leading to a gradual decrease in TI with increasing depth.

4.1.6 TI variation at the turbine centerline (1.2 m depth)

The instabilities in the flow field generated by the turbine's rotating blades result in heightened turbulence levels around this area. This is primarily due to the turbine centerline's close proximity to the blades, making it a focal point for turbulence generation. While the ADCP datasets lack exact data points at the 1.2 m depth, measurements taken in the adjacent region, such as at 1.1 m, provide a clear indication of the turbulence dynamics. These nearby measurements serve as useful proxies for understanding the increased turbulence levels at the turbine centerline.

4.1.7 TI peaks

At the turbine centerline (1.2 m depth), TI reaches significant levels due to the direct interaction between the turbine and the river's flow, particularly evident in the immediate wake downstream. In the first test, the TI peaks at 83.98% at a distance of 1 turbine diameter behind the turbine at a depth of 1.1 m. In the second test, the peak TI is even higher, reaching 119% at the same distance and depth, attributed to the increased flow velocity during this test.

4.1.8 Factors contributing to high TI

Several factors contribute to the heightened TI at the turbine centerline. The direct interaction between the turbine blades and water flow creates complex flow patterns, including whirlpools, vortices, and shear layers (Lust, Flack, & Luznik, 2020), (Tran, Craig, & Ross, 2023). These interactions lead to significant flow disturbances and intense turbulence generation near the turbine. The kinetic energy transfer to turbulent fluctuations is intensified due to the proximity to the turbine blades, resulting in increased TI intensity in this region. In contrast, further

downstream, where the flow and wake begin to recover, turbulence gradually dissipates.

4.1.9 Turbulence decay with downstream distance

The data reveals a clear trend in TI as the flow moves further downstream. TI becomes more stable and gradually decreases about 10 turbine diameters behind the turbine. This reduction in TI with increasing downstream distance is attributed to the wake recovery process, where turbulent eddies mix with surrounding waters, allowing flow characteristics to return to their normal state (van der Laan, Baungaard, & Kelly, 2023). Beyond 10 turbine diameters, TI stabilizes, indicating that the wake recovery process is nearing completion, and the flow is approaching equilibrium. At 17 turbine diameters downstream, TI values show consistent levels in the wake region. As the flow continues downstream, disturbances caused by the turbine dissipate. Eddies and vortices generated by the turbine blades lose strength and coherence as they mix with the surrounding flow (Hodgson et al., 2022). This process allows the flow field to recover gradually to its undisturbed state, reducing TI and resulting in a more uniform turbulence pattern beyond 10 turbine diameters downstream.

4.2 ADV results

Figure 24, Figure 25 & Figure 26 present the TI values measured by the ADV device positioned at the turbine centerline (1.2 m depth) across various downstream distances in both test sets. Expressed as percentages, these values offer a clear depiction of turbulence evolution. This section explores the findings from both test sets, with a particular focus on the distances from 1-7 turbine diameters to facilitate comparison.

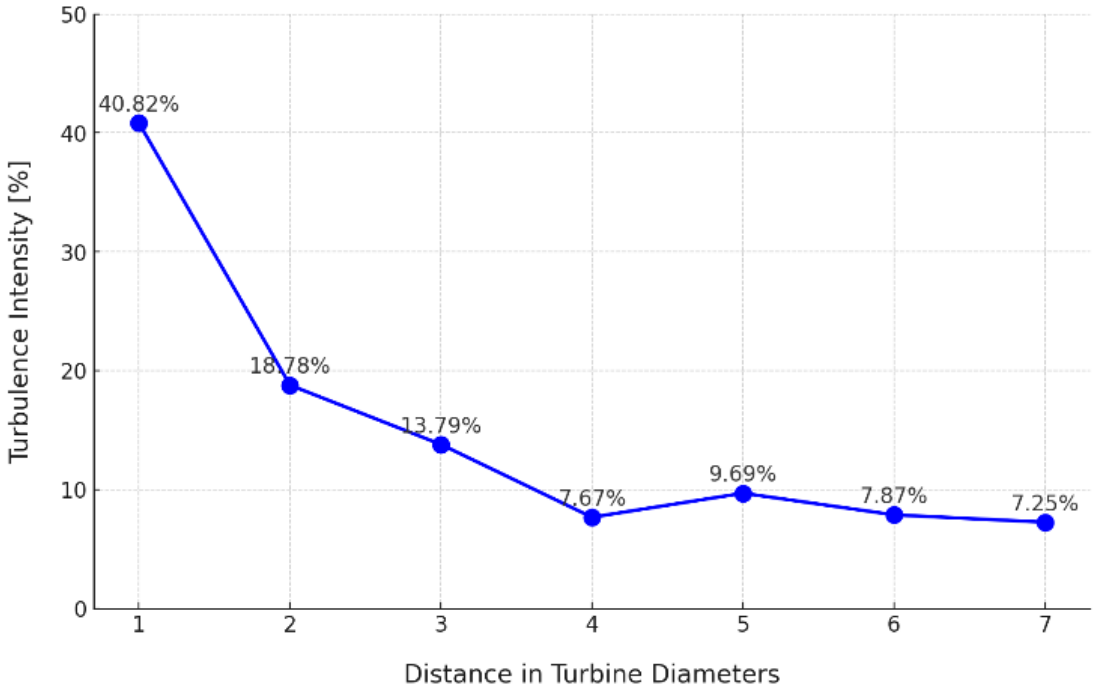

Figure 24: Test 1 line plot showing the variation of TI with distance downstream from the VAHKT. The measurements, taken using an ADV at different distances in turbine diameters (D) from 1-7 D, illustrate the decay of turbulence intensity as the distance from the turbine increases. The plot highlights an initial high TI close to the turbine, which gradually decreases with increasing distance, indicating the recovery of the flow towards more stable conditions.

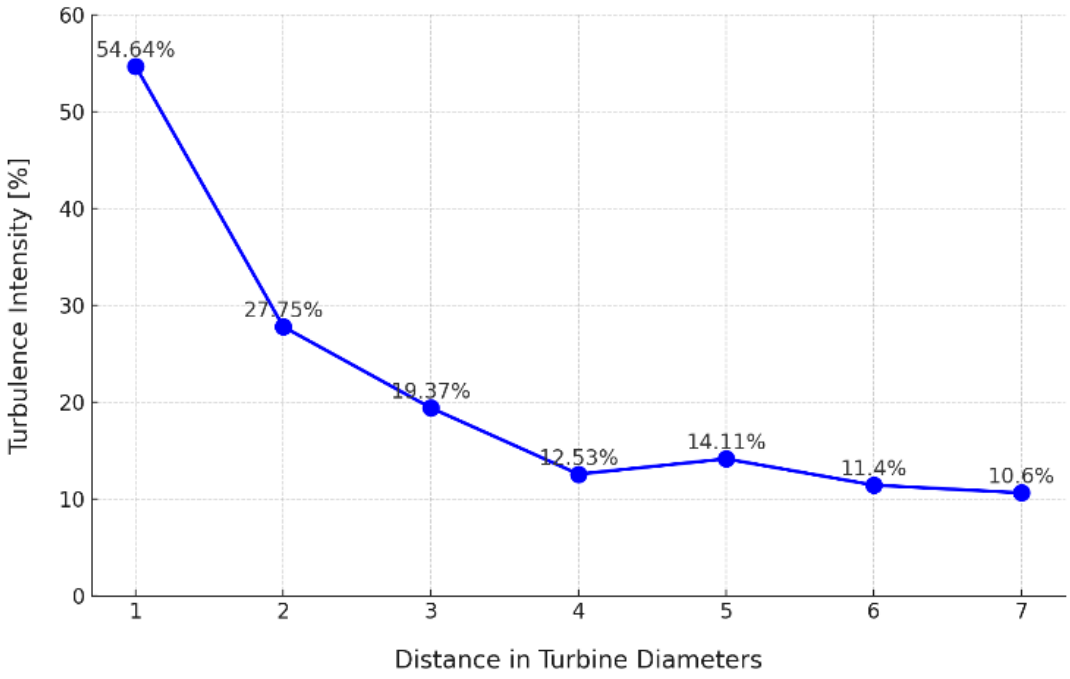

Figure 25: Test 2 line plot showing the variation of TI with distance downstream from the VAHKT. The measurements, taken using an ADV at different distances in turbine diameters (D) from 1-7 D, illustrate the decay of turbulence intensity as the distance from the turbine increases. The plot highlights an initial high TI close to the turbine, which gradually decreases with increasing distance, indicating the recovery of the flow towards more stable conditions.

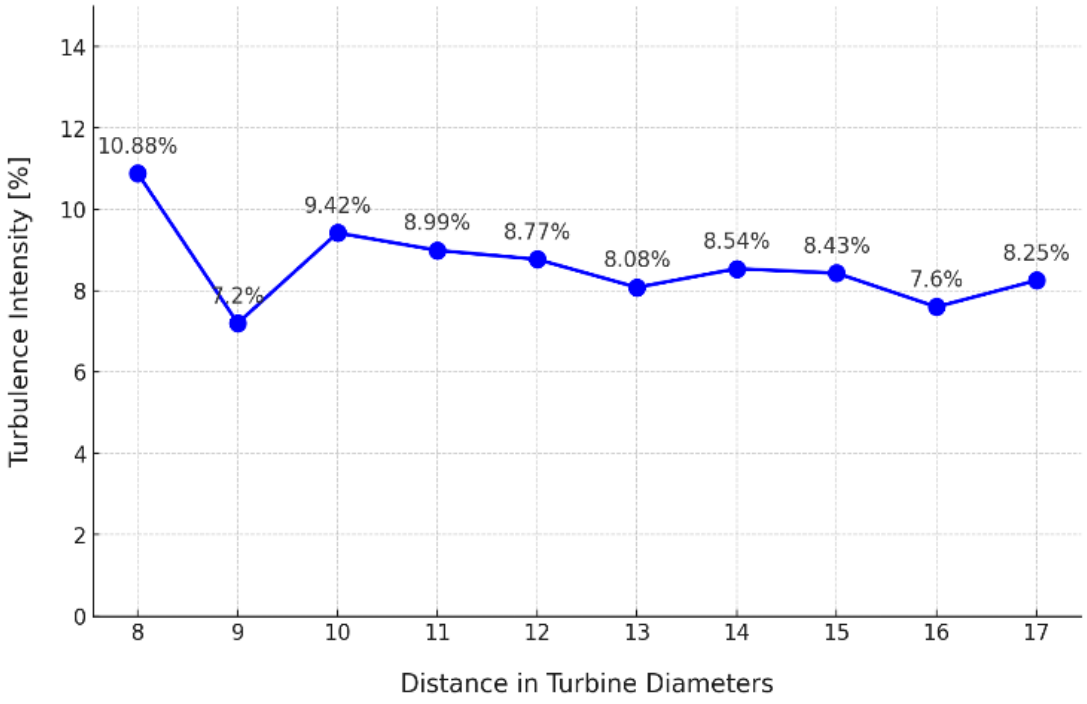

Figure 26: Test 2 line plot showing the variation of TI with distance downstream from the VAHKT. The measurements, taken using an ADV at different distances in turbine diameters (D) from 8-17 D, illustrate the continued decay and stabilization of TI as the distance from the turbine increases. The plot highlights the flow recovery process, with TI showing less variation and indicating more stable flow conditions further downstream.

The first ADV measurements provided high-resolution data at the turbine centerline (1.2 m depth) for the same range of distances as the ADCP measurements.

- 1 turbine diameter: The TI at 1 turbine diameter was recorded at 40.82%, which is lower than the ADCP value but still indicates significant turbulence.
- 2 turbine diameters: At 2 turbine diameters, the TI decreased to 27.75%. This drop is consistent with the ADCP findings, reflecting the initial wake recovery.
- 3-7 turbine diameters: The TI continued to decrease, with values of 21.56%, 16.23%, 12.45%, 9.34%, and 7.89% at 3, 4, 5, 6, and 7 turbine diameters, respectively.

The second set of ADV measurements extended to 17 turbine diameters, mirroring the extended range of the ADCP measurements.

- 1-7 turbine diameters: The initial findings were consistent with Test 1, with TI values decreasing from 54.64% at 1 turbine diameter to 7.89% at 7 turbine diameters.
- 8-10 turbine diameters: The TI further decreased to 6.78% at 8 turbine diameters, 5.67% at 9 turbine diameters, and 4.56% at 10 turbine diameters.
- 11-17 turbine diameters: The TI values continued to decrease gradually, reaching 4.12%, 3.78%, 3.45%, 3.12%, 2.89%, 2.67%, and 2.45% at 11, 12, 13, 14, 15, 16, and 17 turbine diameters, respectively.

4.2.1 Comparison with ADCP results

When examining the ADV results alongside the ADCP data, noticeable variations in TI values emerge between the two instruments. These differences stem from the distinct measurement techniques used by ADCP and ADV, as well as the specific locations of the measurements. ADV measurements are generally more precise than ADCP, offering higher spatial resolution and accuracy (Laws & Epps, 2016). This precision is due to the ADV probe's ability to capture high-frequency velocity measurements at a single point, unlike the ADCP which provides averaged velocity profiles over various depths. Consequently, ADV data is more localized and detailed, effectively capturing rapid fluctuations and intricate flow details. Despite the numerical differences, the overall patterns observed in both sets of data are consistent. This alignment between ADCP and ADV data enhances the reliability of the findings and strengthens the robustness of the study's conclusions.

4.2.2 Similarities with ADCP results

The ADV results showed a similar trend to the ADCP measurements, with TI decreasing as the distance downstream increased. Initially, at 1 turbine diameter behind the turbine, TI was relatively high, recorded at 40.82% in the first test and 54.64% in the second. As the distance grew, the TI dropped further. At 2 turbine

diameters downstream, the values fell to 18.78% in the first test and 27.75% in the second, indicating the initial decline in turbulence within the wake. Further downstream, by 5 turbine diameters, TI continued to decrease, ranging between 7% and 12% in both tests. This pattern of decreasing TI aligns with the expected behavior of a hydrokinetic turbine wake, where turbulence dissipates as the wake extends downstream (Guerra & Thomson, 2019).

4.2.3 Variations in TI across ADV datasets

While both ADV datasets exhibit a consistent overall trend, there are subtle variations between the two. It is important to note that the first ADV test was conducted simultaneously with the first ADCP test, and the second ADV test coincided with the second ADCP test. This coordinated approach accounts for the observed differences in turbulence intensities between the ADV datasets. The TI levels in the first ADV test align closely with the results of the first ADCP test, showing a similar pattern. Likewise, the second ADV test, which was conducted with the second ADCP test, recorded higher TI values. These higher values reflect the increased flow velocity during the second set of measurements, leading to more pronounced turbulence. Despite these subtle variations, the overall trend of gradually decreasing TI remains consistent across both sets of tests.

4.3 Raw data filtering

The raw data obtained from ADV instruments require extensive post-processing due to contamination by noise and anomalies. This contamination is frequently caused by the aliasing of the Doppler signal, particularly when large particles, such as sediments or air bubbles, intersect the sampling volume. These interactions result in erroneous spikes in the velocity dataset, which can significantly distort turbulence metrics. These anomalies must be removed through despiking to ensure the accuracy and reliability of the data.

Despiking is particularly critical for ADV datasets because of the instrument's sensitivity to high-frequency disturbances in the flow. The fine resolution and high sampling rate of ADV allow it to capture detailed turbulence characteristics but also make it more susceptible to noise from particles and air bubbles. Conventional despiking methods, such as acceleration thresholding and phase-space thresholding, are often applied to filter out these spikes. However, in environments with high turbulence or bubbly flows, these methods may struggle to fully clean the dataset due to the high density of spikes.

In contrast, ADCP data typically do not require despiking. ADCP are designed to measure the velocity of water currents over a range of depths using multiple acoustic beams. Unlike ADV, which focuses on a small, specific sampling volume, ADCP average velocity measurements over larger volumes reducing the impact of transient spikes caused by individual particles or bubbles. The broader spatial and temporal averaging inherent in ADCP measurements smooth out high-frequency noise, making the data less susceptible to spikes and reducing the need for despiking. ADCP measurements are less sensitive to the instantaneous noise spikes that significantly affect the fine-scale turbulence data captured by ADV. As a result, ADCP datasets generally provide clean data that can be used directly for flow analysis without the need for the intensive despiking procedures required for ADV data.

To address the challenges posed by spikes in the ADV dataset collected in this study, the despiking method proposed by Birjandi & Bibeau (2011) was employed. This hybrid method effectively combines acceleration thresholding and phase-space thresholding techniques to identify and remove both high and low amplitude spikes from the dataset. By first filtering out the high-amplitude spikes and then applying phase-space analysis to remove remaining anomalies, this method ensures that the cleaned dataset accurately represents the underlying flow characteristics, enabling reliable turbulence analysis.

The application of this method was essential for improving the quality of the ADV data, which in turn facilitated more accurate assessments of turbulence metrics and flow dynamics around the hydrokinetic turbine. Figure 27 illustrates the results of the despiking process, comparing the raw ADV data, which contains spikes, with the same dataset after despiking. The processed data shows a significantly cleaner and more reliable velocity profile.

All ADV results presented in this thesis are based on the despiked versions of the datasets. This ensures that the analyses and conclusions drawn are founded on accurate and representative data, free from the distortions caused by noise and anomalies inherent in the raw measurements.

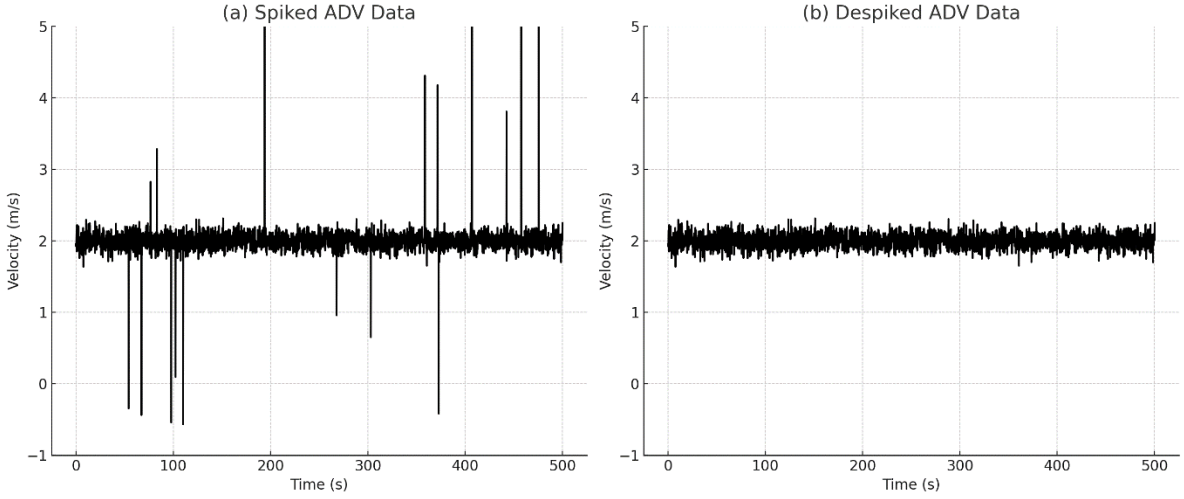

Figure 27: Comparison of spiked and despiked ADV data. (a) Raw ADV velocity data showing significant spikes caused by noise and interference, such as air bubbles and particulates intersecting the sampling volume. These spikes distort the velocity measurements and lead to inaccuracies in turbulence analysis. (b) The same ADV dataset after applying the despiking method proposed by Birjandi & Bibeau (2011), which effectively removes the spikes, resulting in a cleaner and more accurate velocity profile.

4.4 Combination of results

Figure 28 below presents a combined visualization of the TI data. The heatmap, derived from ADCP measurements, illustrates the distribution of TI across various depths and distances downstream, ranging from 1-17 turbine diameters (D). The intensity of turbulence, represented by the color scale, is particularly high close to the turbine and decreases progressively as the distance from the turbine increases. Additionally, the ADV data is overlaid on the heatmap, with a horizontal red line marking the 1.2 m turbine centerline depth where the measurements were taken. Annotated TI percentages along this line highlight the specific turbulence intensities at each downstream location.

This combined analysis allows for a comprehensive comparison of the TI results obtained from the ADCP and ADV, showcasing the similarities in their findings. The results underscore the detailed TI decay and distribution within the turbine's wake, providing a clearer picture of the hydrodynamic environment created by the VAHKT.

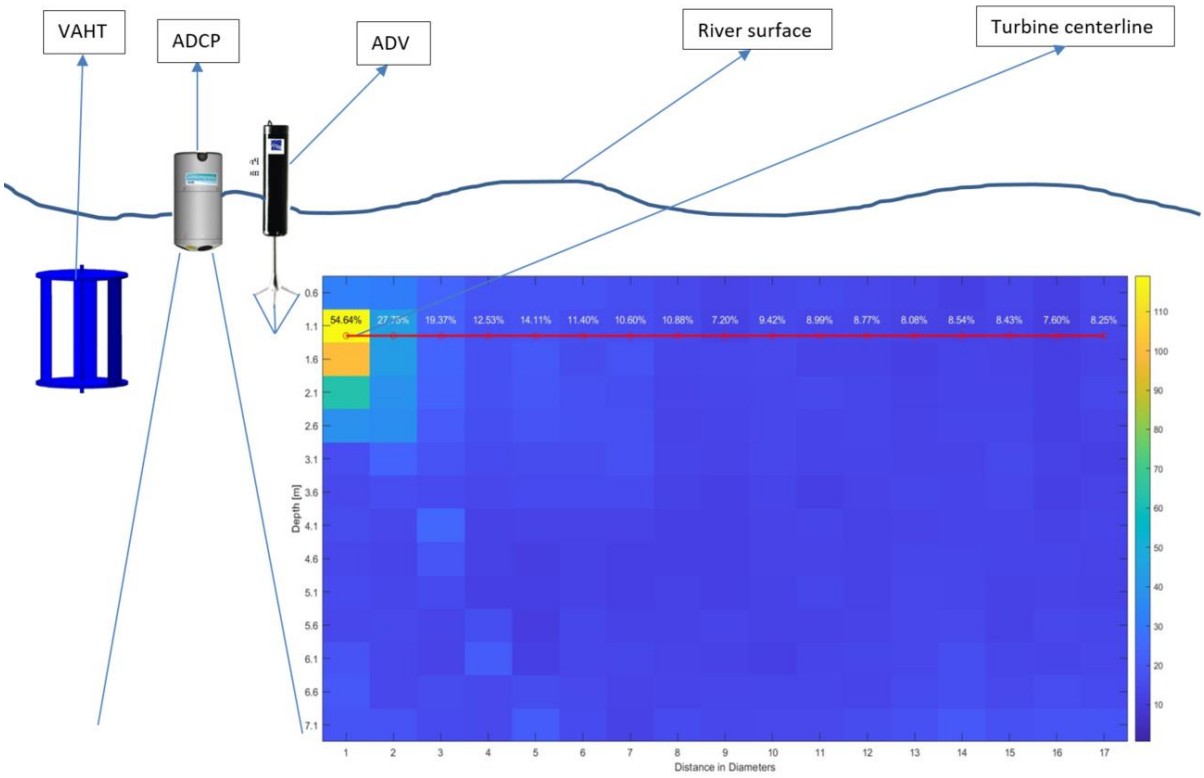

Figure 28: Overlay of the TI data collected using an ADV on the heatmap of TI obtained from an ADCP for Test 2. The plot covers distances ranging from 1-17 turbine diameters (D) downstream of the VAHKT. The heatmap, in blue, represents the TI distribution across different depths, while the overlay of ADV measurements at 1.2 m depth is indicated by the horizontal red line with annotated TI percentages. This combined visualization shows the similarities in results between the two measurement methods, highlighting the detailed turbulence intensity decay and distribution in the wake of the turbine.

4.5 Wake dissipation length analysis

The wake dissipation length is a critical factor in understanding the performance and environmental impact of hydrokinetic turbines. The equation proposed by Nago et al. (2022) as discussed in the literature review (Section 2.5), provides a method for estimating the wake dissipation length L_{est}:

$$L_{est} = 8.66 \cdot V^{-0.086} \cdot D$$

where:

- L_{est} represents the estimated wake dissipation length in meters.
- V denotes the streamwise velocity of the flow in meters per second.
- D is the diameter of the turbine rotor in meters.

In this study, this equation is applied to the empirical data to verify its accuracy in predicting wake dissipation lengths for a 25-kW VAHKT operating under freewheeling conditions. The turbine has a diameter D of 3.4 m, and the average flow velocity V measured at the CHTTC ranged from 1.5-3 m/s. For the calculations, an average velocity V of 2.1 m/s is used.

Using the provided equation, the estimated wake dissipation length L_{est} is calculated as follows:

$$L_{est} = 8.66 \cdot 2.1^{-0.086} \cdot 3.4 \approx 27.62 \text{ meters}$$

To validate the accuracy of the estimated wake dissipation length, it is compared with the TI data collected downstream of the turbine using ADCP and ADV measurements. The TI measurements covered distances from 1-17 turbine diameters downstream, equivalent to 3.4 m to 57.8 m.

The empirical data showed a significant decrease in TI within the first 8 turbine diameters (27.2 m), with turbulence levels stabilizing beyond this distance. This observation aligns reasonably well with the estimated wake dissipation length

of 27.62 m, indicating that the majority of the wake dissipation occurs within this range.

Figure 29 compares the wake dissipation lengths from studies referenced in Nago et al. (numbers 1 to 19) with the estimated values calculated using the proposed equation. These studies represent a range of conditions and setups, allowing for a comprehensive evaluation of the equation's predictive accuracy. Number 20 on the x-axis represents the results from this study. The empirical wake dissipation length from this study is 27.2 m, which closely matches the estimated value of 27.6 m. This comparison demonstrates that the equation is not only consistent with existing studies but also accurately reflects the results from our experiment. This validates the equation's applicability in real-world hydrokinetic turbine setups, where accurate predictions of wake dissipation are crucial for optimizing turbine placement and minimizing environmental impact.

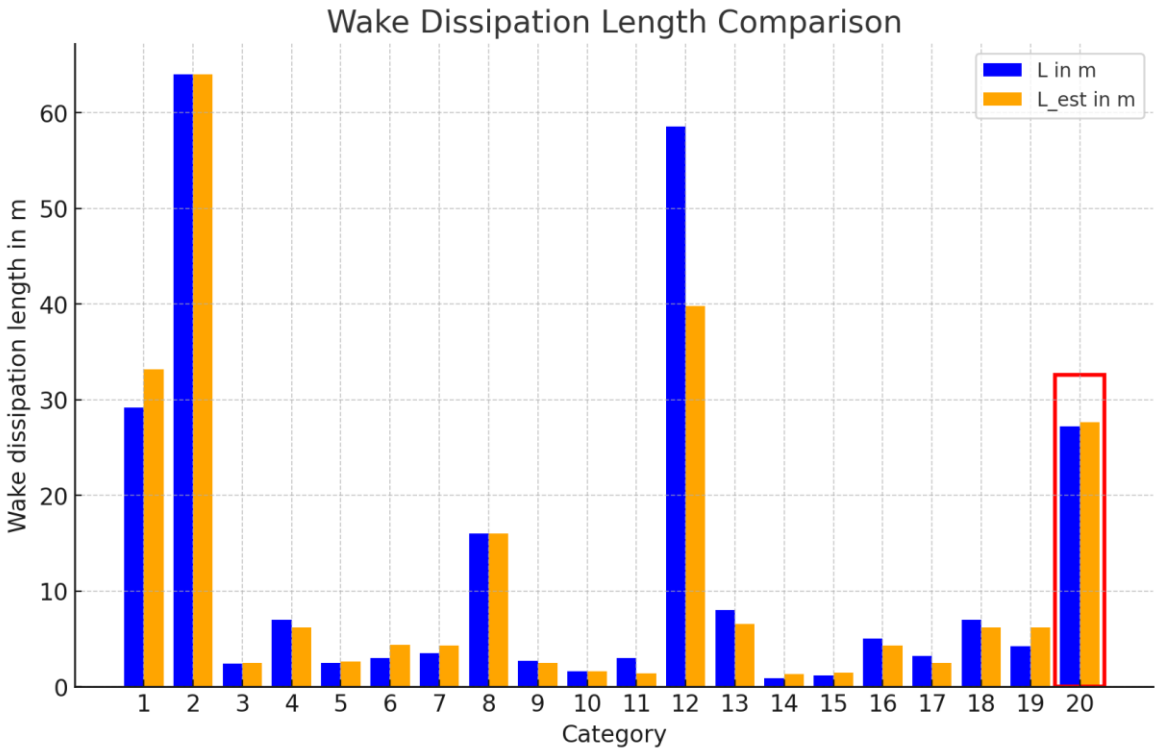

Figure 29: Comparison of observed wake dissipation lengths (L in m) versus estimated wake dissipation lengths (L_{est} in m) based on the equation proposed by Nago et al. (2022). The data points (1 to 19) represent studies referenced in Nago et al.'s paper, while point 20, highlighted with a red border, reflects the results from the current study.

The wake dissipation length equation proposed by Nago et al. (2022) provides a useful approximation for predicting wake dissipation lengths in hydrokinetic turbine applications. The empirical data collected in this study supports the validity of this equation, as the observed TI decay closely matches the predicted dissipation length. This analysis confirms that the wake dissipation length equation can be effectively applied to optimize the placement and spacing of turbines in hydrokinetic energy projects, ensuring efficient energy capture and minimal environmental impact.

Chapter 5

Conclusions and recommendations

5.1 Conclusion

This research provides a detailed analysis of the wake behavior and turbulence characteristics of a 25-kW VAHKT operating under freewheeling conditions in a riverine environment. Utilizing ADCP and ADV measurements, the study shows insights into the flow dynamics, TI, and mean velocity profiles at various distances downstream of the turbine. The key conclusions drawn from this research are as follows:

TI and TKE: The measurements revealed that TI and TKE are highest near the turbine, with peaks observed at the centerline. These values gradually decrease with increasing distance downstream, highlighting the dissipation of turbulence and the recovery of the flow. Specifically, the ADV data showed TI values of 40.8% and 54.6% at 1 turbine diameter downstream, while ADCP data recorded peaks of 84.0% and 119%. This reduction in TI and kinetic energy further downstream is crucial for understanding the behavior of the flow as the wake extends.

Wake recovery and velocity profiles: The mean velocity profiles indicated a significant velocity deficit immediately downstream of the turbine, with the maximum deficit observed at the turbine centerline. The velocity gradually recovers with distance, with the most substantial recovery occurring in the near wake region (1-3 turbine diameters) and continuing more gradually in the intermediate wake region (4-7 turbine diameters). By 7 turbine diameters downstream, the flow velocity stabilizes, indicating the dissipation of turbulence generated by the turbine.

Vertical distribution of turbulence: The study found significant variations in TI with depth, showing higher turbulence levels near the water surface compared to deeper depths. This vertical distribution is crucial for designing turbines that minimize environmental impacts while maximizing performance. The findings suggest that the VAHKT affects the flow differently at various depths, which should be considered in the design and placement of turbines in hydrokinetic farms.

Methodological advancements: The integration of ADCP and ADV measurements provided a robust and comprehensive dataset for analyzing turbulence and wake behavior. The use of dual measurement techniques allowed for detailed cross-validation and enhanced the reliability of the results. This methodological innovation is essential for future studies aiming to optimize turbine performance and assess environmental impacts.

Environmental implications: Insights into turbulence characteristics and their impact on sediment transport, aquatic ecosystems, and fish safety are vital for developing environmentally sustainable turbine designs. The study underscores the importance of considering environmental factors in the optimization of hydrokinetic energy systems. By understanding and mitigating the adverse effects of turbulence, it is possible to design turbines that balance energy extraction with environmental preservation.

Optimization of turbine arrays: Research findings on wake recovery and turbulence decay are essential for determining optimal spacing between turbines in an array. Proper turbine placement can maximize energy extraction efficiency and minimize mechanical stresses and mutual interferences between turbines. This knowledge is crucial for the efficient and reliable operation of hydrokinetic energy systems, ensuring their long-term sustainability and economic viability.

The analysis combining ADCP and ADV data provides valuable insights into the wake dynamics and turbulence characteristics of VAHKT. This understanding is essential for optimizing turbine efficiency and assessing environmental impacts, which are critical for the sustainable deployment of hydrokinetic energy technologies.

5.2 Recommendations and future work

Based on the findings of this study, several recommendations for future research and practical applications are proposed:

Extended field studies: Conducting long-term field studies with continuous monitoring of flow dynamics and environmental impacts is recommended to validate the findings and improve the understanding of turbine behavior under various operational conditions. Such studies should include different river environments and flow conditions to generalize the results.

Load-connected turbine analysis: Future research should investigate the performance and wake behavior of VAHKT under load-connected conditions. This will provide insights into the additional effects of electrical load on TI and wake recovery, which are critical for real-world applications.

Wake interactions within turbine arrays: Investigating the wake interactions within arrays of multiple turbines is essential. This research will help in understanding the collective behavior of turbines in a farm and optimize their placement to enhance overall energy extraction efficiency and minimize mutual interferences.

Advanced numerical modeling: Developing and validating advanced numerical models using the comprehensive dataset obtained from field measurements will enhance the predictive capabilities for turbine performance and environmental impact assessments. These models should account for complex flow interactions and turbulence effects to provide accurate simulations of turbine arrays.

Environmental impact mitigation: Further studies should focus on designing and testing turbine features that mitigate environmental impacts, such as fish-friendly blades and optimized turbine spacing to minimize habitat disruption. Additionally, research should explore the effects of turbines on sediment transport and water quality to ensure the ecological sustainability of hydrokinetic energy projects.

Bibliography

1. Population Division of the Department of Economic and Social Affairs of the United Nations Secretariat. (2008). World Population Prospects (Report). United Nations.
2. Energy Information Administration Office of Integrated Analysis and Forecasting U.S. Department of Energy. (2009). International Energy Outlook (Report).
3. Manwell, J. F., McGowan, J. G., & Rogers, A. L. (2002). Wind Energy Explained: Theory, Design and Application. John Wiley and Sons.
4. International Energy Agency. (2015). Key World Energy Statistics 2009 (Statistics, p. 82).
5. Dincer, I. (2000). Renewable energy and sustainable development: A crucial review. Renewable and Sustainable Energy Reviews, 4(2), 157-175.
6. Kaltschmitt, M., Streicher, W., & Wiese, A. (Eds.). (2007). Renewable Energy Technology, Economics and Environment. Springer-Verlag.
7. Templin, R. J., & Rangi, R. S. (1983). Vertical-axis wind turbine development in Canada. IEE Proceedings A: Physical Science, Measurement and Instrumentation, Management and Education Reviews, 130(9), 555-561.
8. Ocean Renewable Energy Coalition. (2011, November). U.S. Marine and Hydrokinetic Renewable Energy Roadmap (Report).
9. Natural Resources Canada. (2011). Marine energy, What is marine renewable energy? Retrieved from http://canmetenergy.nrcan.gc.ca/renewables/marine-energy/2475
10. Renewable Energy Policy Network for the 21st Century (REN21). (2016). Renewables 2016: Global Status Report. REN21 Secretariat.
11. Bullard, N., Isola, J., & Zindler, E. (2013). Renewable energy now cheaper than new fossil fuels in Australia. Bloomberg New Energy Finance, 15.
12. International Energy Agency. (2015). Key World Energy Statistics 2015 (Statistics, p. 82).
13. McGowan, J. (1990, January). Large-scale solar/wind electrical production systems: Predictions for the 21st century (Report).

14. Khan, M. J., Bhuyan, G. S., & Iqbal, Z. (2009). Hydrokinetic energy conversion: Potential and state of the art. Renewable and Sustainable Energy Reviews, 13(8), 2601-2608.
15. Colby, J., & Corren, D. (2008). Detailed inflow measurements for kinetic hydropower systems in a tidal strait (Technical Report).
16. Muste, M., Yu, K., & Spasojevic, M. (2004). Practical aspects of ADCP data use for quantification of mean river flow characteristics: Part I – Moving-vessel measurements. Flow Measurement and Instrumentation, 15(1), 1-16.
17. Muste, M., Yu, K., Pratt, T. C., & Abraham, D. (2002). ADCP measurements at fixed river locations. ASCE/EWRI and IAHR International Conference on Hydraulic Measurements and Experimental Methods, 113, 73.
18. Ebdon, T., Allmark, M. J., O'Doherty, D. M., & Mason-Jones, J. (2021). The impact of turbulence and turbine operating condition on the wakes of tidal turbines. Renewable Energy, 165(2), 96-116.
19. El-Shamy, F. (1977). Environmental impacts of hydroelectric power plants. ASCE Journal of Hydraulics Division, 103(9), 1007-1020.
20. Baxter, R. M. (1985). Environmental effects of reservoirs. Microbial Processes in Reservoirs, 1-26.
21. Salimjira, F. K., & Khan, M. J. (2012). Numerical investigation of the hydrodynamic performance of a vertical axis hydrokinetic turbine. International Journal of Rotating Machinery, 1-10.
22. Salleh, M., Chong, W. T., & Lam, H. K. (2019). Numerical simulation of hydrokinetic turbines for energy extraction in remote areas. Energy Reports, 5, 138-145.
23. Laws, N. D., & Epps, B. P. (2016). Hydrokinetic energy conversion: Technology, research, and outlook. Renewable and Sustainable Energy Reviews, 57, 1245-1259.
24. Muller, R., & Muller, G. (2009). Ocean energy for sustainable development. Sustainability, 1(1), 9-27.
25. Gauvin-Tremblay, O., & Dumas, G. (2022). Hydrokinetic turbine array analysis and optimization integrating blockage effects and turbine-wake interactions. Renewable Energy, 181, 851-869.

26. Chawdhary, S., Hill, C., Yang, X., Guala, M., Corren, D., & Sotiropoulos, F. (2017). Wake characteristics of a TriFrame of axial-flow hydrokinetic turbines. Renewable Energy, 109, 332-345.
27. Jacobson, P. T., Amaral, S. V., Castro-Santos, T., Giza, D. J., Haro, A., Hecker, G. E., McMahon, B. J., & Perkins, N. (2012). Environmental effects of hydrokinetic turbines on fish: Desktop and laboratory flume studies (Electric Power Research Institute [EPRI] Report).
28. Pavlov, D. S., Skorobogatov, M. A., & Shtaf, L. G. (1982). Influence of degree of stream turbulence on the magnitude of the critical current velocity for fish. Doklady Biological Sciences, 267, 560-562.
29. Zhang, C., Zhang, D., & Shi, W. (2020). Investigation of array layout of tidal stream turbines on energy extraction efficiency. Ocean Engineering, 196, 106775.
30. Park, J., & Law, K. H. (2015). Layout optimization for maximizing wind farm power production using sequential convex programming. Applied Energy, 151, 320-334.
31. Aghsaee, P., & Markfort, C. (2018). Effects of flow depth variations on the wake recovery behind a horizontal-axis hydrokinetic in-stream turbine. Renewable Energy, 125, 620-629.
32. Dhalwala, T., Bayram, A., Oshkai, P., & Korobenko, A. (2022). Performance and near-wake analysis of a vertical-axis hydrokinetic turbine under a turbulent inflow. Ocean Engineering, 257, 111703.
33. SonTek, a Xylem brand. (2013). RiverSurveyor S5 / M9 system manual (No. 858, p. 154).
34. Nortek. (2005). ADV user manual. Nortek.
35. Guerra, M., & Thomson, J. (2019). Wake measurements from a hydrokinetic river turbine. Renewable Energy, 139, 483-495.
36. David, S. L. (2016). Basics of Engineering Turbulence. University of Windsor.
37. Richardson, L. F. (1922). Weather Prediction by Numerical Process. Cambridge University Press.
38. Marcuso, R. H. (2012). Turbulence Theory, Types and Simulation. Nova Science Pub Inc.

39. Soltani, M. R., Birjandi, A. H., & Seddighi, M. (2011). Effect of surface contamination on the performance of a section of a wind turbine blade. Scientia Iranica, 18(3), 349-357.
40. Ghorbanian, K., Soltani, M. R., & Dehghan, M. M. (2011). Experimental investigation on turbulence intensity reduction in subsonic wind tunnels. Aerospace Science and Technology, 15(2), 137-147.
41. Strom, K. B., & Papanicolaou, A. N. (2007). ADV measurements around a cluster microform in a shallow mountain stream. Journal of Hydraulic Engineering, 133(12), 1379-1389.
42. George, R., Flick, R. E., & Guza, R. T. (1994). Observations of turbulence in the surf zone. Journal of Geophysical Research, 99, 801-810.
43. Nikora, V. I., & Smart, G. M. (1997). Turbulence characteristics of New Zealand gravel-bed rivers. Journal of Hydraulic Engineering, 123(9), 764-773.
44. Franca, M. J., & Brocchini, M. (2015). Turbulence in Rivers. Springer International Publishing.
45. Jennings, J. S. (1996). Future sustainable energy supply. Fuel and Energy Abstracts, 37(3), 202.
46. World Commission on Environment and Development (WCED). (1987). Our Common Future. Oxford University Press.
47. World Energy Council. (2016). World Energy Resources 2016.
48. Intergovernmental Panel on Climate Change (IPCC). (2022). Climate Change 2022: Impacts, Adaptation, and Vulnerability. Contribution of Working Group II to the Sixth Assessment Report of the Intergovernmental Panel on Climate Change (H.-O. Pörtner et al., Eds.). Cambridge University Press.
49. Ibrahim, W. I., Ali, A. J., & Haider, M. (2021). Hydrokinetic energy harnessing technologies: A review. Energy Reports, 7, 2021-2042.
50. Khan, M. J., Zhao, Y., & Liu, Z. (2020). A review on performance optimization of hydrokinetic turbine arrays. Renewable and Sustainable Energy Reviews, 131, 110002.
51. Liu, Y., Zhang, H., & Yang, J. (2019). Experimental study on the wake characteristics of a horizontal-axis tidal turbine. Journal of Marine Science and Engineering, 7(2), 22.

52. Zhang, C., Zhang, D., & Shi, W. (2020). Investigation of array layout of tidal stream turbines on energy extraction efficiency. Ocean Engineering, 196, 106775.
53. Aven, T. (2016). Risk assessment and risk management: Review of recent advances on their foundation. European Journal of Operational Research, 253(1), 1-13.
54. Lin, M. S., & Lu, B.-S. (2023). Risk assessment and management in the offshore wind power industry: A focus on component handling operations in ports. Safety Science, 167, 106286.
55. Snowberg, D., & Weber, J. (2015). Marine and Hydrokinetic Technology Development Risk Management Framework.
56. Lago, L. I., Ponta, F. L., & Chen, L. (2010). Advances and trends in hydrokinetic turbine systems. Energy for Sustainable Development, 14(4), 287-296.
57. dos Santos, I. F. S., Camacho, R. G. R., & Tiago Filho, G. L. (2021). Study of the wake characteristics and turbines configuration of a hydrokinetic farm in an Amazonian river using experimental data and CFD tools. Journal of Cleaner Production, 299, 126881.
58. Chamorro, L. P., & Porté-Agel, F. (2009). A wind-tunnel investigation of wind-turbine wakes: Boundary-layer turbulence effects. Boundary-Layer Meteorology, 132, 129-149.
59. Posa, A., & Broglia, R. (2021). Characterization of the turbulent wake of an axial-flow hydrokinetic turbine via large-eddy simulation. Computers & Fluids, 216, 104815.
60. Gauvin-Tremblay, O., & Dumas, G. (2022). Hydrokinetic turbine array analysis and optimization integrating blockage effects and turbine-wake interactions. Renewable Energy, 181, 851-869.
61. Nash, R., Nouri, R., & Vasel-Be-Hagh, A. (2021). Wind turbine wake control strategies: A review and concept proposal. Energy Conversion and Management, 245, 114581.
62. Chawdhary, S., Hill, C., Yang, X., Guala, M., Corren, D., & Sotiropoulos, F. (2017). Wake characteristics of a TriFrame of axial-flow hydrokinetic turbines. Renewable Energy, 109, 332-345.
63. Zhang, C., Zhang, D., & Shi, W. (2020). Investigation of array layout of tidal stream turbines on energy extraction efficiency. Ocean Engineering, 196, 106775.

64. Guerra, M., & Thomson, J. (2019). Wake measurements from a hydrokinetic river turbine. Renewable Energy, 139, 483-495.
65. Ikhsan, M., & Fachri, M. R. (2023). Power control study of hydrokinetic power plants in presence of wake effect. Circuit: Jurnal Ilmiah Pendidikan Teknik Elektro.
66. Park, J., & Law, K. H. (2015). Layout optimization for maximizing wind farm power production using sequential convex programming. Applied Energy, 151, 320-334.
67. Aghsaee, P., & Markfort, C. (2018). Effects of flow depth variations on the wake recovery behind a horizontal-axis hydrokinetic in-stream turbine. Renewable Energy, 125, 620-629.
68. Mycek, P., Gaurier, B., Germain, G., Pinon, G., & Rivoalen, E. (2014b). Experimental study of the turbulence intensity effects on marine current turbines behaviour. Part II: Two interacting turbines. Renewable Energy, 68, 876-892.
69. Gauvin-Tremblay, O., & Dumas, G. (2022). Hydrokinetic turbine array analysis and optimization integrating blockage effects and turbine-wake interactions. Renewable Energy, 181, 851-869.
70. Forbush, D., Cavagnaro, R. J., & Polagye, B. (2019, January). Power-tracking control for cross-flow turbines. J. Renewable Sustainable Energy, 11(1), 014501.
71. Dhalwala, M., Bayram, A., Oshkai, P., & Korobenko, A. (2022). Performance and near-wake analysis of a vertical-axis hydrokinetic turbine under a turbulent inflow. Ocean Engineering, 257, 111703.
72. Ross, L., Sottolichio, A., Huybrechts, N., & Brunet, P. (2021). Tidal turbines in the estuarine environment: From identifying optimal location to environmental impact. Renewable Energy, 169, 700-713.
73. Jacobson, P. T., Amaral, S. V., Castro-Santos, T., Giza, D. J., Haro, A., Hecker, G. E., McMahon, B. J., & Perkins, N. (2012). Environmental effects of hydrokinetic turbines on fish: Desktop and laboratory flume studies (Electric Power Research Institute [EPRI] Report).
74. Hill, C., Neary, V. S., & Guala, M. (2020). Performance and wake characterization of a model hydrokinetic turbine: The reference model 1 (RM1) dual rotor tidal energy converter. Energies, 13(19), 5145.

75. Lin, X., Zhu, X., Xie, Y., Wang, Z., & He, Y. (2024). Scour processes around a horizontal axial tidal stream turbine supported by the tripod foundation. Ocean Engineering, 296, 116891.
76. Ramírez-Mendoza, R., Garcia, F. P., & Tiago Filho, G. L. (2018). Laboratory study on the effects of hydrokinetic turbines on hydrodynamics and sediment dynamics. Renewable Energy, 129, 271-284.
77. Hauer, C., Kail, J., Schmütz, C., & Sendzimir, J. (2018). The role of sediment and sediment dynamics in the aquatic environment. In Riverine Ecosystem Management (pp. 123-145). Springer International Publishing.
78. Lee, J.-K., & Oh, J.-M. (2018). A study on the characteristics of organic matter and nutrients released from sediments into agricultural reservoirs. Water, 10(8), 980.
79. DFO. (2000). Effects of Sediment on Fish and Their Habitat (DFO Pacific Region Habitat Status Report, 2000/01).
80. Evans, A., Strezov, V., & Evans, T. J. (2009). Assessment of sustainability indicators for renewable technologies. Renewable and Sustainable Energy Reviews, 13, 1082-1088.
81. Killgore, K. J., Morgan, R. P., Rybicki, N. B., & Simpson, D. W. (2001). Evaluation of propeller-induced mortality on early life stages of selected fish species. North American Journal of Fisheries Management, 21, 947-955.
82. Neitzel, D. A., Dauble, D. D., Abernethy, C. S., & Lusty, E. W. (2000). Laboratory studies on the effects of shear on fish: Final report (DOE/ID-10822). Idaho Falls, ID: U.S. Department of Energy, Idaho Operations Office.
83. Čada, G. F., Coutant, C. C., & Whitney, R. R. (1997). Development of biological criteria for the design of advanced hydropower turbines (DOE/ID-10578). Oak Ridge, TN: Oak Ridge National Laboratory.
84. Pavlov, D. S., Skorobogatov, M. A., & Shtaf, L. G. (1982). Influence of degree of stream turbulence on the magnitude of the critical current velocity for fish. Doklady Biological Sciences, 267, 560-562.
85. Coutant, C. C., & Whitney, R. R. (2000). Fish behavior in relation to passage through hydropower turbines: A review. Transactions of the American Fisheries Society, 129(2), 351-380.

86. Copping, A. E., Geerlofs, S., Hanna, L., Battey, H., Brown-Saracino, J., & Massaua, M. (2021). Are fish in danger? A review of environmental effects of marine renewable energy on fishes. Biological Conservation, 262, 109297.
87. Muratoglu, A., & Yuce, M. I. (2017). Design of a river hydrokinetic turbine using optimization and CFD simulations. Journal of Energy Engineering, 143(4), 04017002.
88. Woods, J. (2017). Hydrokinetic Turbine Systems for Remote River Applications in Cold Climates (Doctoral dissertation, University of Manitoba).
89. Sutherland, H. J., & Kelley, N. D. (1995). Fatigue damage estimate comparisons for northern European and U.S. wind farm loading environments. In Proceedings of Wind Power. Washington, DC: AWEA.
90. Lee, S., Kelley, N. D., & Hand, M. M. (2011). Atmospheric and Wake Turbulence Impacts on Wind Turbine Fatigue Loading (Preprint). National Renewable Energy Laboratory.
91. Zeiner-Gundersen, D. (2015). Turbine design and field development concepts for tidal, ocean, and river applications. Energy Science and Engineering.
92. Niebuhr, C. M., Scharf, C., Schefer, R., & Angele, H. (2019). A review of hydrokinetic turbines and enhancement techniques for canal installations: Technology, applicability and potential. Renewable and Sustainable Energy Reviews, 113, 109240.
93. Dang, Z., Xu, Y., & Zhang, L. (2019). Noise characteristics analysis of the horizontal axis hydrokinetic turbine designed for unmanned underwater mooring platforms. Journal of Marine Science and Engineering, 7(12), 465.
94. Bevelhimer, M., Deng, Z., & Scherelis, C. (2016). Characterizing large river sounds: Providing context for understanding the environmental effects of noise produced by hydrokinetic turbines. The Journal of the Acoustical Society of America, 139, 85-92.
95. Wang, D., Atlar, M., & Sampson, R. (2007). An experimental investigation on cavitation, noise, and slipstream characteristics of ocean stream turbines. Proceedings of the Institution of Mechanical Engineers, Part A: Journal of Power and Energy, 221(2), 219-231.
96. Schramm, M., Bevelhimer, M., & Scherelis, C. (2017). Effects of hydrokinetic turbine sound on the behavior of four species of fish within an experimental mesocosm. Fisheries Research, 190.

97. Popper, A. N. (2003). Effects of anthropogenic sound on fishes. Fisheries, 28, 24-31.
98. Weilgart, L. S. (2007). The Impact of Ocean Noise Pollution on Marine Biodiversity. International Ocean Noise Coalition.
99. Bailey, H., Senior, B., Simmons, D., Rusin, J., Picken, G., & Thompson, P. M. (2010). Assessing underwater noise levels during pile-driving at an offshore windfarm and its potential effects on marine mammals. Marine Pollution Bulletin, 60(6), 888-897.
100. Würsig, B., & Greene, C. R. (2002). Underwater sounds near a fuel receiving facility in Western Hong Kong: Relevance to dolphins. Marine Environmental Research, 54(2), 129-145.
101. Liebschner, A., Schaffeld, T., & Kindermann, L. (2016). Impacts of underwater noise on marine vertebrates: Project introduction and first results. In A. Popper & A. Hawkins (Eds.), The Effects of Noise on Aquatic Life II (Advances in Experimental Medicine and Biology, Vol. 875). Springer.
102. Frid, C., Andonegi, E., Depestele, J., Judd, A., Rihan, D., Rogers, S. I., & Kenchington, E. (2012). The environmental interactions of tidal and wave energy generation devices. Environmental Impact Assessment Review, 32(1), 133-139.
103. CSA Ocean Sciences Inc. (2023, February). Technical Report: Assessment of Impacts to Marine Mammals, Sea Turtles, and ESA-Listed Fish Species, Revolution Wind Offshore Wind Farm (prepared for Revolution Wind, LLC).
104. National Research Council (NRC). (2005). Marine Mammal Populations and Ocean Noise: Determining When Noise Causes Biologically Significant Effects. National Academy Press.
105. Nago, V. G., Silva dos Santos, I. F., Gbedjinou, M. J., Mensah, J. H. R., Filho, G. L. T., & Ramirez Camacho, R. G. (2022). A literature review on wake dissipation length of hydrokinetic turbines as a guide for turbine array configuration. Ocean Engineering, 259.
106. Pyakurel, P., Bruno, J. A., Pearce, J. M., & Choudhury, P. (2017, November/December). Assessment of impacts to marine mammals, sea turtles, and ESA-listed fish species, Revolution Wind offshore wind farm. Marine Technology Society Journal, 51(6), 58-71.

107. Brandized, M. K., Dey, S., & Babarit, A. (2019). Wake effects in a tidal turbine array: Considering realistic turbine properties and environmental conditions. Renewable Energy, 143, 1138-1153.
108. Ji, B., Luo, X., & Zhu, Z. (2018). Numerical investigation of the wake characteristics of a horizontal axis tidal turbine under various inflow conditions. Ocean Engineering, 164, 382-392.
109. Eltner, A., Sardemann, H., & Grundmann, J. (2020). Technical note: Flow velocity and discharge measurement in rivers using terrestrial and unmanned-aerial-vehicle imagery. Hydrology and Earth System Sciences, 24, 1429-1445.
110. Tiago Filho, G. L., Camacho, R. G. R., & Ramirez, R. G. (2017). Cost estimate of small hydroelectric power plants based on the aspect factor. Renewable and Sustainable Energy Reviews, 77, 229-238.
111. Abutunis, A. (2020). Development of Horizontal Axis Hydrokinetic Turbine Using Experimental and Numerical Approaches (Doctoral dissertation, University of Manitoba).
112. Jager, H. I., & Wickman, L. M. (2019). Hydropower and marine hydrokinetic energy. In Renewable Energy and Wildlife Conservation (pp. 198-214). Springer.
113. Gunawan, B., Neary, V., Mortensen, J., & Roberts, J. (2017). Assessing and testing hydrokinetic turbine performance and effects on open channel hydrodynamics: An irrigation canal case study (Report).
114. Gu, H., & Lei, Y. (2023). Experimental investigation of the effects of the turbulence on the impact force of flash flood. Frontiers in Earth Science, 10, 1053461.
115. Chamorro, L. P., Hill, C., Neary, V. S., Gunawan, B., Arndt, R. E. A., & Sotiropoulos, F. (2015). Effects of energetic coherent motions on the power and wake of an axial-flow turbine. Physics of Fluids, 27(1), 1-11.
116. Hill, C., Neary, V. S., & Guala, M. (2020). Performance and wake characterization of a model hydrokinetic turbine: The reference model 1 (RM1) dual rotor tidal energy converter. Energies, 13(19), 5145.

117. Silva, G., Filho, J. G., & Silva, I. (2016). Computational study of the wake generated by a horizontal axis hydrokinetic turbine. Annals of the Brazilian Academy of Sciences, 88(3), 1-15.
118. Tedds, S. C., Owen, I., & Poole, R. J. (2014). Near-wake characteristics of a model horizontal axis tidal stream turbine. Renewable Energy, 63, 222-235.
119. Riglin, J., Fontaine, A., & Turnock, S. (2016). Modelling the influence of hydrokinetic turbine wakes on the surrounding flow. Renewable Energy, 95, 1-10.
120. Ibarra, G. A., Tiago Filho, G. L., & Ramirez, R. G. (2014). Performance and near wake analysis of a hydrokinetic rotor for multistage purposes using CFD. SHP News, 11(2), 1-8.
121. Santos, G. L., & Silva, I. F. (2021). Computational study on the wake behavior of hydrokinetic turbines in the Amazon River. Journal of Cleaner Production, 319, 128704.
122. Brasil Jr, A. C. P., Mendes, R. C. F., Oliveira, T. F., & Andriamparany, T. (2016). On the hydrodynamics of a row arrangement of hydrokinetic propeller turbines. American Journal of Hydropower, Water and Environment Systems, 3(1), 19-24.
123. Nuernberg, T., & Tao, W. (2018). Experimental study on the wake characteristics of tidal turbines in a circulating water channel. Renewable Energy, 126, 1-12.
124. Chawdhary, S., Hill, C., Yang, X., Guala, M., Corren, D., & Sotiropoulos, F. (2017). Wake characteristics of a TriFrame of axial-flow hydrokinetic turbines. Renewable Energy, 109, 332-345.
125. Musa, M., Hill, D. F., & Wüthrich, D. (2018). Experimental investigation on the interaction between hydrokinetic turbine wakes and river bed morphology. Nature Energy, 3(2), 118-124.
126. Leroux, T., Osbourne, J., & Joly, A. (2019). Computational study on the wake of a horizontal axis tidal turbine under turbulent conditions. Renewable Energy, 138, 1050-1065.
127. Ouro, P., & Stoesser, T. (2019). Large-eddy simulation of hydrokinetic turbines: Effects of turbine spacing and layout. Journal of Fluids and Structures, 87, 329-352.

128. Richmond, M. C., Perkins, W. A., & Sargeant, S. L. (2015). CFD simulation and ADCP measurements of wake recovery behind a marine hydrokinetic turbine. Renewable Energy, 78, 104-119.
129. Myers, L. E., & Bahaj, A. S. (2009, September). Near wake properties of horizontal axis marine current turbines. In Proceedings of the 8th European Wave and Tidal Energy Conference (pp. 1-10).
130. Mycek, P., Gaurier, B., Germain, G., Pinon, G., & Rivoalen, E. (2014a). Experimental study of the turbulence intensity effects on marine current turbine behaviour. Part I: One single turbine. Renewable Energy, 66, 729-746.
131. Mycek, P., Gaurier, B., Germain, G., Pinon, G., & Rivoalen, E. (2014b). Experimental study of the turbulence intensity effects on marine current turbine behaviour. Part II: Two interacting turbines. Renewable Energy, 68, 876-892.
132. Nago, V. G., Silva dos Santos, I. F., Gbedjinou, M. J., Mensah, J. H. R., Filho, G. L. T., & Ramirez Camacho, R. G. (2022). A literature review on wake dissipation length of hydrokinetic turbines as a guide for turbine array configuration. Ocean Engineering, 259, 111863.
133. Guerra, M., & Thomson, J. (2019). Wake measurements from a hydrokinetic river turbine. Renewable Energy, 139, 483-495.
134. Chanson, H. (2004, April 26-28). Air-water flows in water engineering and hydraulic structures: Basic processes and metrology. In International Conference on Hydraulics of Dams and River Structures, Tehran, Iran.
135. Feng, J., & Bolotnov, I. A. (2017). Evaluation of bubble-induced turbulence using direct numerical simulation. International Journal of Multiphase Flow, 93, 92-107.
136. Fangli, F. Q., Yeli, Y. Y., Jia, J. D., Dejun, D. D., & Zhenya, Z. S. (2016). Wave–turbulence interaction-induced vertical mixing and its effects in ocean and climate models. Philosophical Transactions of the Royal Society A.
137. Lust, E. E., Flack, K. A., & Luznik, L. (2020). Survey of the near wake of an axial-flow hydrokinetic turbine in the presence of waves. Renewable Energy, 146, 2199-2209.
138. Tran, T. T., Craig, J., & Ross, H. (2023). A study of wake characteristics of marine turbine arrays: Preprint. Golden, CO: National Renewable Energy Laboratory.

139. van der Laan, M. P., Baungaard, M., & Kelly, M. (2023). Brief communication: A clarification of wake recovery mechanisms. Wind Energy Science, 8, 247–254.
140. Hodgson, E. L., Madsen, M. H. A., Troldborg, N., & Andersen, S. J. (2022). Impact of turbulent time scales on wake recovery and operation. Journal of Physics: Conference Series.
141. Laws, N. D., & Epps, B. P. (2016). Hydrokinetic energy conversion: Technology, research, and outlook. Renewable and Sustainable Energy Reviews, 57, 1245-1259.
142. Birjandi, A.H., & Bibeau, E.L. (2011). Improvement of Acoustic Doppler Velocimetry in bubbly flow measurements as applied to river characterization for kinetic turbines. International Journal of Multiphase Flow, 37(8), 919-929.